Role of amphiregulin in mediating the bone anabolic actions of parathyroid hormone

von

Freya Franziska Jay

Inaugural-Dissertation zur Erlangung der Doktorwürde
der Tierärztlichen Fakultät der Ludwig-Maximilians-Universität München

Role of amphiregulin in mediating the bone anabolic actions of parathyroid hormone

von

Freya Franziska Jay

aus Bruchsal

München 2016

Aus dem
Veterinärwissenschaftlichen Department der Tierärztlichen Fakultät
der Ludwig-Maximilians-Universität München

Lehrstuhl für Molekulare Tierzucht und Biotechnologie

Arbeit angefertigt unter der Leitung von:

Priv.-Doz. Dr. Marlon R. Schneider

Gedruckt mit der Genehmigung der Tierärztlichen Fakultät

der Ludwig-Maximilians-Universität München

Dekan:	Univ.-Prof. Dr. Joachim Braun
Berichterstatter:	Priv.-Doz. Dr. Marlon R. Schneider
Korreferent:	Univ.-Prof. Dr. Dušan Palić

Tag der Promotion: 16. Juli 2016

Contents

Abbreviations

aa	aminoacids
ADAM	a disintegrin and metalloproteinase
ANOVA	analysis of variance
APES	3-aminopropyltriethoxysilane
AREG	amphiregulin
BFR	bone formation rate
BMD	bone mineral density
bp	base pair
B.Pm	bone perimeter
BS	bone surface
BTC	betacellulin
BV	bone volume
COL1	collagen α1 promoter
Cre	causes recombination
Crea	creatinine
Ct.Ar	cortical area
CTF	cytosolic fragment
Ct.Th	cortical thickness
DPD	deoxypyridinoline
Dsk5	dark skin 5
E	embryonic day
Ec.BPm	endocortical bone perimeter
EDTA	ethylenediaminetetraacetate
e.g.	*exempli gratia*
EGF	epidermal growth factor
EGFR	epidermal growth factor receptor
EGR	early growth response
EIA	enzyme immunoassay
ELISA	enzyme-linked immunosorbent assay
EPGN	epigen
EREG	epiregulin

FELASA	Federation of European Laboratory Animal Science Associations
GH	growth hormone, somatotropin
GMCSF	granulocyte-macrophage colony-stimulating factor
G-protein	guanine nucleotide-binding protein
GRB2	growth factor receptor-bound protein 2
h	hour / hours
HBEGF	heparin-binding EGF-like growth factor
HoleAr	hole area
HoleNo	hole number
HolePm	hole perimeter
IGF1	insulin-like growth factor 1
IL	interleukin
KO	knockout
L1	first lumbar vertebra
loxP	locus of crossing-over
Ma.Ar	marrow area
MAPK	mitogen-activated protein kinase
MAR	mineral apposition rate
MCF	Michigan Cancer Foundation
MCP1	monocyte chemoattractant protein 1
MCSF	macrophage colony-stimulating factor
min	minute / minutes
MMA	methylmethacrylate
MMP	matrix metalloproteinase
MMRRC	The Mutant Mouse Regional Resource Center
mRNA	messenger ribonucleic acid
NF-κb	nuclear factor-kappa b
N.Oc	number of osteoclasts
N.Tb	number of trabeculae
Ob.S	osteoblast surface
O.Th	osteoid thickness
OV	osteoid volume
PBS	phosphate buffered saline
PCR	Polymerase chain reaction

PI3K	phosphatidylinositol 3’kinase
PKA	protein kinase A
PKC	protein kinase C
PLC	phospholipase C
pQCT	Peripheral quantitative computed tomography
Pro-AREG	“pro-form” of amphiregulin, amphiregulin precursor
Ps.BPm	periosteal bone perimeter
PTH	parathyroid hormone
PTHrP	parathyroid hormone related peptide
RANK	receptor activator of nuclear factor-kappa b
RANKL	receptor activator of nuclear factor-kappa b ligand
RUNX2	Runt-related transcription factor 2
Scid	severe combined immunodeficiency
SEM	standard error of the mean
SH2	Src-homology-2
siRNA	small interfering ribonucleic acid
SNK test	Student-Newman-Keuls test
SOS	son of sevenless
STAT	signal transducer and activator of transcription
TACE	tumor-necrosis factor alpha converting enzyme
TAE buffer	Tris-acetate-EDTA-buffer
T.Ar	tissue area
Tb.Ar	trabecular area
Tb.N	trabecular number
Tb.Sp	trabecular separation
Tb.Wi	trabecular width
TGFA	transforming growth factor alpha
TRAP	tartrate-resistant acid phosphatase
TRIS	Tris(hydroxymethyl)aminomethane
Tt.Ar	total area
TtCross-sectAr	total cross-sectional area
TV	tissue volume
Wa5	waved 5
WT	wild-type control

1 Introduction

The bone is a complex organ that fulfils a great variety of functions including mechanical support, protection of vital organs, regulation of blood calcium levels and hematopoiesis sustenance. To perform these multiple functions, bone tissue is constantly remodeled in a cyclical renewal process, where bone resorption by osteoclasts is continuously counterbalanced by osteoblastic bone formation (Schneider *et al.*, 2009b).

Parathyroid hormone (PTH) is a major endocrine regulator of bone remodeling and calcium homeostasis (Poole and Reeve, 2005, Schneider *et al.*, 2009b). It is secreted by the parathyroid glands in response to low extracellular calcium levels and, after binding to the PTH-receptor on its target cells, it activates several signaling cascades (Poole and Reeve, 2005, Swarthout *et al.*, 2002). PTH raises the reduced blood calcium levels by stimulating bone resorption, tubular calcium re-absorption in the kidney and synthesis of 1,25-dihydroxyvitamin D_3, thus increasing the calcium uptake in the small intestine. In addition to this classical bone catabolic action, PTH can also act as a bone anabolic agent and significantly increase the bone mineral density (BMD) when administered intermittently (Hock *et al.*, 1988, Poole and Reeve, 2005, Tam *et al.*, 1982).

Although many signaling pathways and molecules have been identified to be key factors in mediating the bone anabolic effect of intermittent PTH, the detailed mechanisms have not yet been fully understood. There is accumulating evidence that amphiregulin (AREG), one ligand of the epidermal growth factor receptor (EGFR), is involved in mediating the bone anabolic effect of intermittent PTH (Schneider *et al.*, 2009b, Schneider and Wolf, 2009).

Areg is significantly upregulated in osteoblastic cells and bone tissue after PTH treatment and was therefore identified as a PTH-regulated target gene both *in vivo* and *in vitro* (Qin *et al*., 2005). Expression of *Areg* can also be modulated by other osteotropic hormones, such as 1,25-dihydroxyvitamin D_3 and prostaglandin E_2 (Qin *et al.*, 2005). Furthermore, release of AREG by osteoblastic cells after PTH treatment increases the recruitment of bone marrow mesenchymal progenitors via PI3K/Akt and p38MAPK

pathways and subsequently promotes their migration towards the bone surface (Zhu *et al.*, 2012). The bone anabolic effect of intermittent PTH was blunted in osteoblast-specific EGFR-knockout mice (Zhu *et al.*, 2012). Moreover, female mice lacking AREG have less trabecular bone as compared to their controls (Qin *et al.*, 2005). Vice versa, mice overexpressing *Areg* specifically in osteoblasts revealed a transient increase in trabecular bone mass (Vaidya *et al.*, 2015). Hence, these data indicate that AREG seems to be the main EGFR ligand mediating the bone anabolic effect of PTH.

To clarify to which extent AREG is required for the bone anabolic actions of PTH, we treated AREG deficient and control female mice at an age of 12 weeks intermittently with PTH or vehicle (physiological saline) for four weeks and examined their bone phenotype in detail.

2 Review of literature

Epidermal growth factor receptor

The epidermal growth factor receptor (EGFR, HER1, ERBB1) is a transmembrane tyrosine kinase receptor that can be activated by seven ligands: amphiregulin (AREG) (Berasain and Avila, 2014), betacellulin (BTC) (Dahlhoff *et al.*, 2014), epidermal growth factor (EGF) (Zeng and Harris, 2014), epigen (EPGN) (Schneider and Yarden, 2013), epiregulin (EREG) (Riese and Cullum, 2014), heparin-binding EGF-like growth factor (HBEGF) (Taylor *et al.*, 2014) and transforming growth factor α (TGFA) (Singh and Coffey, 2014). Once bound by a ligand, the EGFR forms homodimers with another EGFR molecule or heterodimers with one of the closely related receptors ERBB2 (HER2, NEU), ERBB3 (HER3) or ERBB4 (HER4) (Citri and Yarden, 2006). In addition, the EGFR can be transactivated via other receptors, such as G-protein-coupled receptors (also known as seven transmembrane-domain receptors), whose activation lead to cleavage of the membrane-bound ligand precursors (Yarden and Sliwkowski, 2001, Prenzel *et al.*, 1999, Tao and Conn, 2014). The ligands of the four ERBB receptors can be divided into three groups: The first group binds exclusively to the EGFR and includes AREG, EGF, EPGN and TGFA. The second group includes BTC, EREG and HBEGF and binds both the EGFR and ERBB4. The neuregulins (NRG1 – NRG4) are representing the third group. NRG1 and NRG2 bind both ERBB3 and ERBB4, whereas NRG3 and NRG4 only bind to ERBB4 (Arteaga and Engelman, 2014). ERBB2 has no known ligand, but it is the preferred dimerization partner of the other ERBB receptors, and is able to amplify their signaling (Citri and Yarden, 2006, Yarden and Sliwkowski, 2001).

Phosphorylation of the receptor dimers on specific tyrosine residues of the intracellular tails leads to the recruitment of a number of signal transducers, such as the Src-homology-2 (SH2) and growth factor receptor-bound protein 2 (GRB2), which initiate the recruitment of RAS and the activation of mitogen-activated protein kinase (MAPK) pathways. Other important pathways are the phosphatidylinositol 3'kinase (PI3K-AKT) pathway, the phospholipase Cγ-protein kinase C (PLC-PKC) pathway and the signal transducer and activator of transcription (STAT) 1, 3 and 5 (Citri and Yarden, 2006, Schneider *et al.*, 2009b, Yarden and Sliwkowski, 2001).

Most mice lacking EGFR die at mid-gestation or birth, but they may survive up to post-natal day 20 depending on their genetic background. Surviving EGFR-Knockout mice are growth retarded, have an impaired epithelial development and show abnormalities in several organs, including skin, kidney, brain and bone (Citri and Yarden, 2006, Miettinen *et al.*, 1995, Sibilia and Wagner, 1995, Threadgill *et al.*, 1995).

Egfr overexpression has been described in several tumor types, e.g. in lung and pancreas, and EGFR inhibitors, such as the monoclonal antibody cetuximab, are used successfully in cancer therapy (Citri and Yarden, 2006, Arteaga and Engelman, 2014).

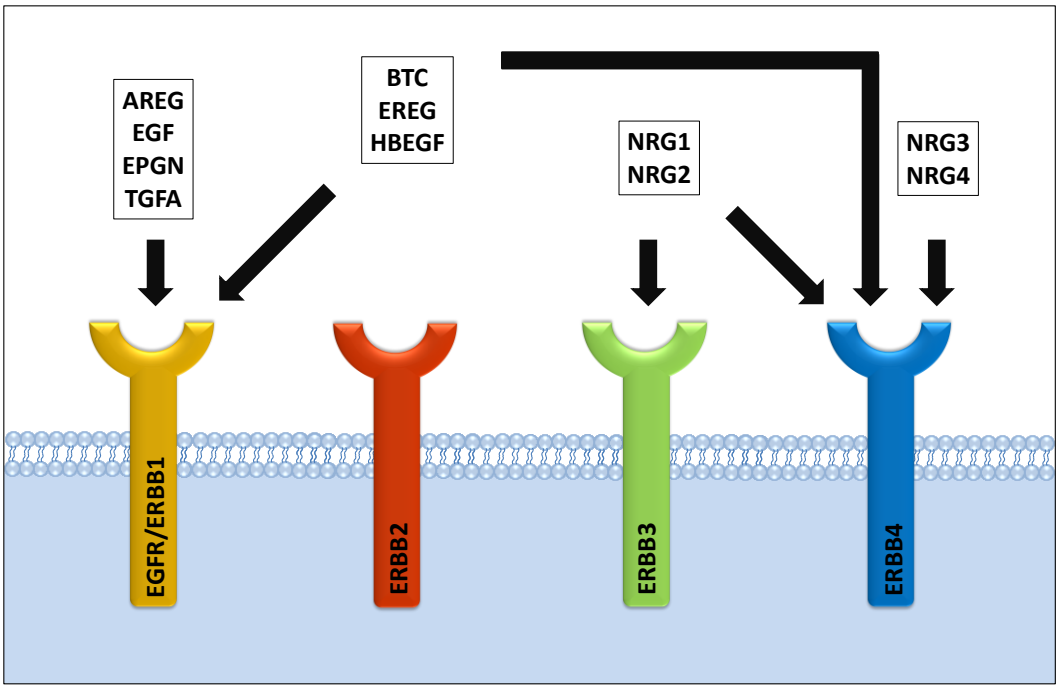

Figure 1 Simplified schematic overview of the binding specificities of the ERBB receptor ligands. AREG, EGF, EPGN and TGFA specifically bind to EGFR, whereas BTC, EREG and HBEGF bind both EGFR and ERBB4. ERBB2 has no known ligand. NRG1 and NRG2 bind both ERBB3 and ERBB4, whereas NRG3 and NRG4 only bind to ERBB4.

Amphiregulin

AREG was first identified in the serum-free conditioned medium of MCF-7 human breast carcinoma cells treated with phorbol 12-myristate 13-acetate (Shoyab *et al.*, 1988). AREG was described as a bifunctional growth factor, with the ability to inhibit the growth of several human carcinoma cells and at the same time to stimulate the growth of human fibroblasts and other cells (Shoyab *et al.*, 1988, Berasain and Avila, 2014), a capacity which led to its name. Today AREG is known as one ligand of the EGFR and is therefore mainly involved in regulating cell proliferation and differentiation (Schneider and Wolf, 2009, Harris *et al.*, 2003).

Areg is expressed as a type I transmembrane glycoprotein precursor (Pro-AREG) of 252 aminoacids (Fitch *et al.*, 2003). The soluble form of AREG (78-84 aa) is formed via proteolytic cleavage of Pro-AREG by the membrane-bound tumor necrosis factor alpha converting enzyme (TACE), which belongs to the disintegrin and metalloprotein-ase family (ADAM17) (Berasain *et al.*, 2007, Harris *et al.*, 2003, Hinkle *et al.*, 2004, Sahin *et al.*, 2004, Sunnarborg *et al.*, 2002). Mature AREG contains the EGF motif and can activate the EGFR in a paracrine or autocrine manner, but the EGFR can also be activated by Pro-AREG via juxtacrine interactions or via exosomes expressing Pro-AREG (Higginbotham *et al.*, 2011, Singh and Harris, 2005, Willmarth and Ethier, 2006). Additionally, it was shown that Pro-AREG and the AREG-cytosolic fragment (AREG-CTF) generated after AREG cleavage can be internalized into the nucleus and may be responsible for part of AREG effects (Berasain and Avila, 2014, Isokane *et al.*, 2008).

Areg is expressed in many tissues, including lung, heart, spleen, kidney, pancreas, colon, testis, placenta, ovary and breast (Plowman *et al.*, 1990). Recently, AREG was found in human colostrum (Nojiri *et al.*, 2012).

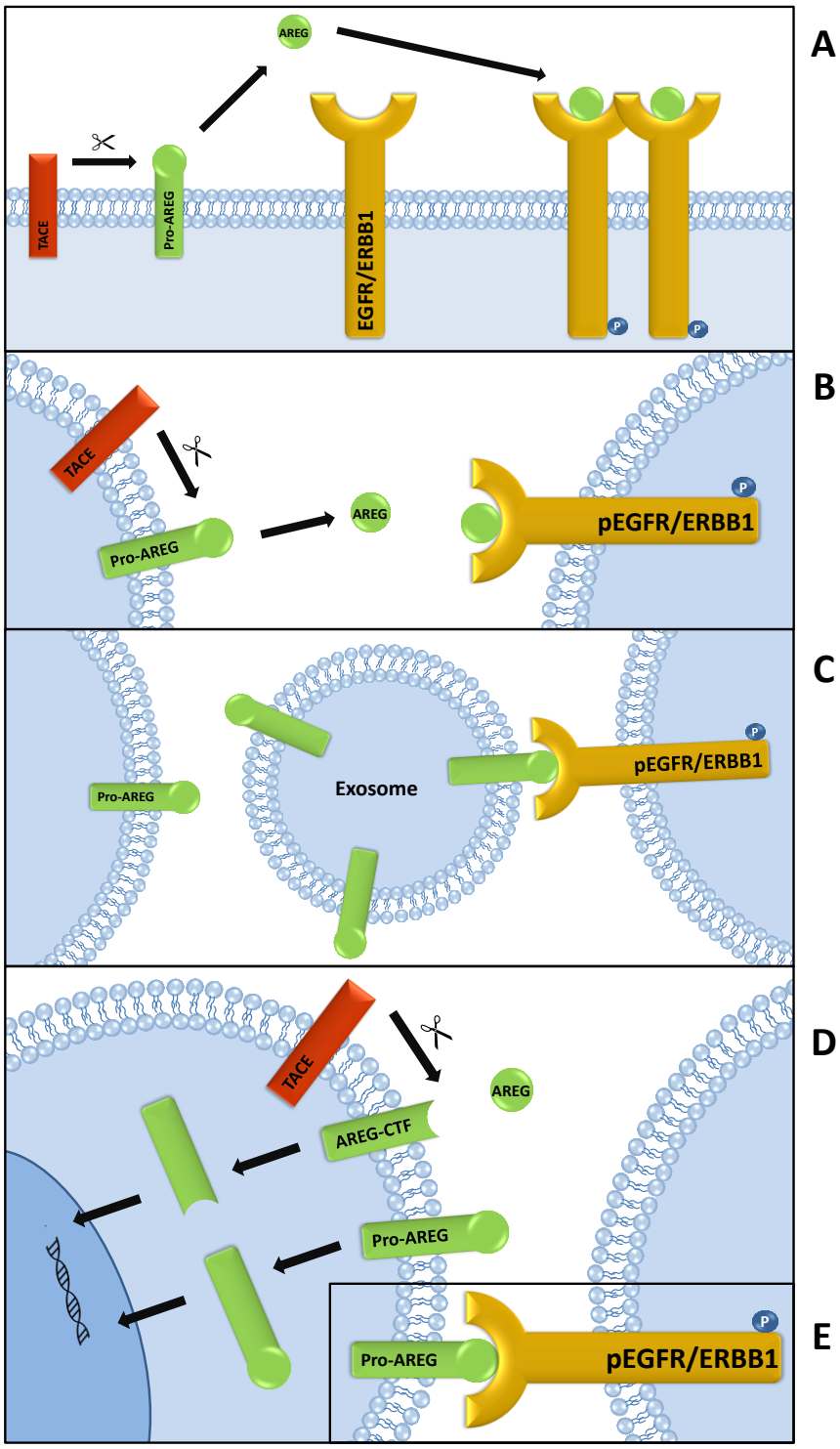

Figure 2 Schematic overview of AREG processing and signaling. TACE-mediated proteolytic cleavage of Pro-AREG leads to the soluble form of AREG, which can activate the EGFR via autocrine (**A**) or paracrine (**B**) signaling. **C** Exosomes expressing Pro-AREG can activate the EGFR via paracrine signaling. **D** Pro-AREG and the AREG cytosolic fragment (AREG-CTF) can also, at least in part, mediate AREG effects via intracellular signaling. **E** Membrane-bound Pro-AREG can bind the EGFR of neighboring cells and therefore signal via juxtacrine interactions.

Mice lacking AREG are viable and fertile, but show an impaired mammary gland development (Luetteke *et al.*, 1999), develop mucosal lesions in the fundus of the stomach (Nam *et al.*, 2009) and, although *Areg* expression in the healthy liver is very low, show signs of liver damage (Berasain *et al.*, 2005). It is reported that AREG-KO mice have less trabecular bone as compared to their control littermates (Qin *et al.*, 2005). Mice overexpressing *Areg* in basal keratinocytes show a psoriasis-like phenotype (Cook *et al.*, 1997), and most recently it was demonstrated that osteoblast-specific *Areg* overexpression leads to a transient anabolic effect in long bones (Vaidya *et al.*, 2015).

Areg is overexpressed in several cancer types, e.g. breast, lung, liver, stomach, pancreas and colon. AREG has intrinsic tumor-promoting activities and can stimulate cellular invasion and increase cell motility (Busser *et al.*, 2011). Most recently it was shown that increased *Areg* expression promotes migration of human osteosarcoma cell lines *in vitro* and cell metastasis and tumor progression of osteosarcoma *in vivo* (Liu *et al.*, 2015).

Under inflammatory conditions *Areg* is expressed in several immune cells, and it plays important roles in tissue repair and wound healing (Zaiss *et al.*, 2015). For instance, AREG plays a pivotal role in the protection from liver injury (Berasain *et al.*, 2005).

Bone

The bone is a complex organ that, unlike most organs, is not restricted to one location or structure, but rather spread over the whole body in several uniquely shaped elements (Karsenty and Wagner, 2002). Bone tissue has several functions, including mechanical support for muscles, protection of vital organs, regulation of blood calcium levels, and sustenance of hematopoiesis. To fulfill these functions, bone tissue is constantly remodeled in a cyclical process, where bone resorption by osteoclasts is constantly counterbalanced by bone formation by osteoblasts (Schneider *et al.*, 2009b).

Bone development begins with mesenchymal cell condensations, which differentiate into chondrocytes and then form a cartilaginous template. The innermost chondrocytes further differentiate into hypertrophic chondrocytes, which attract blood vessels and direct mineralization of the adjacent extracellular matrix before they die through apoptosis. Osteoclasts and capillaries invade the remaining mineralized extracellular matrix,

which is then replaced by bone in a process called endochondral ossification. Later, during longitudinal growth, this process becomes restricted to the growth plates. In some cases the mesenchymal condensations skip the cartilaginous step and directly differentiate into osteoblasts. This process is called intramembranous ossification and occurs in a few body areas, e.g. the flat bones of the skull (Karsenty and Wagner, 2002, Schneider *et al.*, 2009b).

Osteoblasts are the major bone forming cells, which produce several extracellular proteins, including alkaline phosphatase, osteocalcin and type I collagen. The collagen-rich extracellular matrix built by osteoblasts is termed osteoid. Osteoblasts can become inactive bone lining cells or, when entombed within extracellular matrix, osteocytes, which are important regulators of bone remodeling. Osteocytes produce sclerostin, which mainly inhibits the WNT signaling in osteoblasts and therefore promotes their differentiation (Long, 2012).

Osteoclasts are bone specific multinucleated cells derived from the monocyte/macrophage haematopoietic lineage. They attach to the bone and secrete acid and lytic enzymes, e.g. tartrat-resistant acid phosphatase (TRAP), to resorb the bone matrix. The receptor activator of NF-κb ligand (RANKL) is a key factor for osteoclast differentiation and activation. It can be expressed by osteoblasts to stimulate bone resorption via binding to its receptor RANK (receptor activator of NF-κb) on the surface of osteoclasts, which means that osteoblasts can directly regulate osteoclasts. Another protein regulating osteoclast activity is osteoprotegerin (OPG), which acts as a decoy receptor for RANKL and therefore blocks osteoclast formation (Boyle *et al.*, 2003).

Long bones can be divided in three regions: The midshaft (diaphysis), the metaphyses (below the growth plates) and the epiphyses (above the growth plates). The diaphysis consists mainly of dense cortical bone, which surrounds the bone marrow cavity. The metaphysis and epiphysis are composed of trabecular (cancellous) bone (Clarke, 2008).

Role of EGFR in skeletal biology and pathology

The EGFR plays an important role in bone development and homeostasis (Schneider *et al.*, 2009b). Mice lacking the EGFR are growth retarded and have facial deformities, including elongated snouts, underdeveloped mandibulae and a high incidence of cleft palate (Miettinen *et al.*, 1995, Miettinen *et al.*, 1999). EGFR-KO mice have an impaired trabecular bone formation, a delayed endochondral ossification and an enlarged zone of hypertrophic chondrocytes in the growth plate of long bones on embryonic days 16.5 and 18.5 and on postnatal day 1 (Sibilia *et al.*, 2003, Wang *et al.*, 2004). Calvarial osteoblasts from EGFR-KO mice show decreased proliferation and increased differentiation, indicating that normal EGFR signaling in osteoblasts accelerates proliferation, but inhibits differentiation, thus keeping osteoblasts in an undifferentiated, pre-mature state (Sibilia *et al.*, 2003). Furthermore, EGFR-KO mice showed a delayed recruitment of osteoclasts into the hypertrophic cartilage (Wang *et al.*, 2004).

Due to the early lethality of EGFR-KO mice, the role of EGFR in bone biology at later time points could not be characterized. To circumvent this problem, mouse models with an extended survival time were generated, including conditional knockout models using the Cre/loxP system and treatment of mice with tyrosine kinase inhibitors or EGFR antibodies.

Zhang and co-workers generated preosteoblast/osteoblast-specific EGFR-KO mice using the Cre/loxP system (Zhang *et al.*, 2011b). In these mice the loxP (floxed) sequences are flanking exon 3 of the *Egfr* gene, and Cre-mediated recombination results in a frameshift and two stop codons in exon 4. $EGFR^{flox/flox}$ Col 3.6-Cre mice developed no bone phenotype as compared to controls, probably due to residual EGFR activity. To further reduce this activity the mice were crossbred with Waved 5 mice (Wa5), which contain a point mutation leading to a kinase dead dominant-negative EGFR (Lee *et al.*, 2004). 3-month-old $EGFR^{Wa5/flox}$ Col 3.6-Cre mice had a significantly reduced total and trabecular bone mineral density (BMD) and their femurs were shorter and thinner. Additionally, WT mice treated with the EGFR inhibitors gefitinib or erlotinib showed a bone phenotype similar to that of $EGFR^{Wa5/flox}$ Col 3.6-Cre mice, indicating that signaling via the EGFR leads to an anabolic effect in bone (Zhang *et al.*, 2011b). This was also confirmed in the same study using Dsk5 mice, in which constitutively activation of the EGFR leads to an increased signaling, and therefore to a higher BMD

(Fitch *et al.*, 2003, Zhang *et al.*, 2011b). Furthermore, Zhang and co-workers investigated the bone phenotype of heterozygous Wa5 mice in a 129S1/SvImJ background, but there were no differences in 1 and 3 months of age (Zhang *et al.*, 2011b). Shortly afterwards it was reported that in a different genetic background (C57BL/6), heterozygous Wa5 mice at the age of 3 months have a significantly reduced total BMD in femurs and lumbar vertebral bodies (Schneider *et al.*, 2012).

Additionally, Zhang and co-workers treated 1-month-old rats with the EGFR inhibitor gefitinib and these rats exhibited an accumulation of hypertrophic chondrocytes in the growth plate as compared to their vehicle treated controls. Osteoclast recruitment was reduced due to a decreased *Rankl* expression in gefitinib-treated rats. Furthermore, gefitinib treatment led to a decreased expression of matrix metalloproteinases (MMP9, MMP13, MMP14) (Zhang *et al.*, 2011a).

To generate a chondrocyte-specific EGFR-KO mouse, Zhang and co-workers used the same strategy as before, with one Wa5 and one floxed *Egfr* allele, but a type 2 collagen promoter-driven Cre (Col2-Cre) (Zhang *et al.*, 2011a). $EGFR^{Wa5/flox}$ Col2-Cre mice had an enlarged zone of hypertrophic chondrocytes and a delayed formation of the secondary ossification center, due to a suppressed excavation of cartilage canals from the perichondrium into the cartilage and a reduced expression of matrix metalloproteinases (MMPs) and *Rankl* in the hypertrophic chondrocytes, which also leads to a delayed differentiation, mineralization and apoptosis of these cells (Zhang *et al.*, 2013).

Osteoclasts do not express functional *Egfr*, but its ligands can stimulate osteoclast formation indirectly by modulating the expression levels of the osteoclast regulatory factors *Opg* and monocyte chemoattractant protein 1 (MCP1) in osteoblasts. EGF-like ligands can stimulate the expression of *Mcp1* in osteoblasts, which leads to an increased osteoclast activity, and they can inhibit the expression of *Opg* (Zhu *et al.*, 2007).

Overexpression of EGFR ligands in mice leads to ligand-specific effects on bone formation (Schneider *et al.*, 2009b). Mice overexpressing a shortened human EGF precursor are growth retarded, show an increased proliferation and abnormal accumulation of osteoblasts in the periosteum and endosteum, and have a reduced cortical thickness as compared to controls (Chan and Wong, 2000). Overexpression of *Btc* in mice results in round heads, a reduced longitudinal bone growth, and an increased

cortical BMD in the appendicular skeleton, which is mainly due to an increased endocortical bone apposition (Schneider *et al.*, 2009a, Schneider *et al.*, 2005). An osteoblast-specific overexpression of *Areg* under the control of the 2.3kb collagen α1 promoter leads to a transient increase in the trabecular bone mass (Vaidya *et al.*, 2015), and, conversely, female mice lacking AREG have less trabecular bone as compared to their controls (Qin *et al.*, 2005).

RT-PCR analysis confirmed the expression of *Areg*, *Btc*, *Egf*, *Ereg*, *Hbegf* and *Egfr* and *Erbb2* in osteoblasts (Qin *et al.*, 2005).

In vitro studies with the mouse preosteoblastic cell line MC3T3, mouse bone marrow osteoblastic cells, and human bone marrow stromal stem cells, revealed that EGF-like ligands stimulate osteoblast proliferation and suppress their differentiation and mineralization; furthermore, EGFR signaling inhibits the expression of two important osteoblast-specific transcription factors: *Runx2* and *Sp7* (osterix) (Zhu *et al.*, 2011). Microarray analysis of osteoblastic cells treated with EGF revealed an immediate increase in the mRNA expression levels of the transcription factors *Egr1*, *2* and *3* with a peak after 30 min in MCT3 cells and after 1 h in rat calvarial osteoprogenitors, and EGR2 was identified to be a key mediator for EGF-induced cell proliferation and survival (Chandra *et al.*, 2013).

Egfr expression is upregulated in bone and soft tissue tumors (Dobashi *et al.*, 2007), in osteosarcoma-derived cell lines and in osteosarcomas (Wen *et al.*, 2007). More importantly, EGFR is upregulated in tumors that have a high tendency to metastasize to bone, such as breast, lung and prostate cancer (Citri and Yarden, 2006, Di Lorenzo *et al.*, 2002, Mishra *et al.*, 2011, Schneider *et al.*, 2009b). Treatment with tyrosine kinase inhibitors decreased the growth of human renal carcinoma cells implanted into tibiae of nude mice (Weber *et al.*, 2003), inhibited the osteolytic bone destruction in tibiae inoculated with a human non-small lung cancer cell line in Scid mice (Furugaki *et al.*, 2011), and reduced the number of bone metastases of prostate carcinoma (Angelucci *et al.*, 2006). Knockdown of the *Egfr* expression in nude mice with intratibial inoculation of bone metastatic breast cancer cells overexpressing *Areg* reduced the tumor growth within the bone (Nickerson *et al.*, 2012). These data underline the prominent role of EGFR signaling in bone metastases development.

The major mechanism of osteolytic bone destruction in patients with bone metastases is tumor-mediated stimulation of bone resorption (Roodman, 2001). EGFR activation in cancer cells leads to the production of signaling molecules such as PTHrP (PTH related peptide). PTHrP binds the PTH receptor, which leads to an increased *Rankl* expression and therefore stimulates osteoclast activation and differentiation. Interestingly, while AREG was identified as the major EGFR ligand controlling *Pthrp* expression in breast cancer cells, blocking autocrine EGFR signaling loops with an AREG antibody only resulted in a modestly inhibited motility of breast cancer cells (Gilmore *et al.*, 2008, Nickerson *et al.*, 2012).

Recently, it was shown by Liu and co-workers that *Areg* is upregulated in two human osteosarcoma cell lines (MG63 and U2OS). Furthermore, supplementation of AREG increases the migration of these osteosarcoma cells and AREG enhances tumor progression and cell metastasis of osteosarcoma *in vivo*, whereas *Areg* knockdown reduced the number of pulmonary metastases (Liu *et al.*, 2015).

Parathyroid hormone

Parathyroid hormone (PTH) is the major hormonal regulator of bone remodeling and calcium homeostasis. PTH is secreted as an 84 aa polypeptide by the parathyroid glands in response to low extracellular calcium levels, and binds after being processed at its target cells to the PTH receptor, a G-protein-coupled receptor, thus activating distinct signaling pathways, e.g. the protein kinase A (PKA) and protein kinase C (PKC) pathways (Partridge *et al.*, 2006, Poole and Reeve, 2005). PTH acts on the bone to stimulate bone resorption and to increase the release of calcium (Poole and Reeve, 2005, Swarthout *et al.*, 2002). It indirectly stimulates osteoclasts by increasing the expression of *Rankl* in stromal cells and osteoblasts (Teitelbaum, 2000). In the kidney, PTH increases tubular calcium re-absorption and synthesis of 1,25-dihydroxyvitamin D_3, which then enhances the calcium uptake in the intestine. Paradoxically, in addition to this classical bone catabolic action, PTH can also act as a bone anabolic agent, depending on the pattern of administration. While continuous infusion causes bone loss, daily injections of PTH increase bone formation (Poole and Reeve, 2005, Tam *et al.*, 1982). Teriparatide, a recombinant 1-34 aa peptide of human PTH, is currently used as a treatment for patients with osteoporosis (Sugiyama *et al.*, 2015).

The detailed mechanisms behind the anabolic actions of PTH have not yet been fully understood. Intermittent injections of PTH increase the number of osteoblasts by stimulating their proliferation and differentiation (Nishida *et al.*, 1994, Pettway *et al.*, 2008), attenuating their apoptosis (Bellido *et al.*, 2003, Jilka *et al.*, 1999) and activating bone lining cells (Dobnig and Turner, 1995). Over the years several signaling pathways have been identified to play an important role in mediating this effect (Schneider *et al.*, 2012), including insulin-like growth factor-1 (IGF1) (Miyakoshi *et al.*, 2001), c-fos (Demiralp *et al.*, 2002), interleukin-18 (Raggatt *et al.*, 2008), ß-arrestin 2 (Bouxsein *et al.*, 2005) and sclerostin (Kramer *et al.*, 2010a).

Microarrays were used to access PTH-regulated genes in bone (Qin *et al.*, 2003, von Stechow *et al.*, 2004) and to compare gene expression profiles between intermittent and continuous PTH (1-34) treatment (Onyia *et al.*, 2005). In both treatments Oniya and co-workers found increased levels of genes associated with bone formation. Continuous PTH treatment of rats led to higher expression of genes associated with bone turnover and osteoclast formation, such as MMPs and cathepsin K. Intermittent PTH treatment led to fewer changes in gene expression levels, and most of the regulated genes are associated with receptor binding (e.g. IGF-binding protein 6), immune response or catalysis (e.g. carboxypeptidase E). The latter gene was also upregulated after continuous PTH treatment, although to a lesser extent. Surprisingly, some genes uniquely regulated by intermittent PTH treatment are associated with neuronal tissue (Onyia *et al.*, 2005). Shortly afterwards, Li and co-workers presented similar results (Li *et al.*, 2007a). Li and co-workers compared gene expression profiles of rats treated continuously or intermittently with three different PTH peptides. Intermittent injections of PTH (1-31) or PTH (1-34) led to an increased bone formation, whereas PTH (3-34) did not. PTH (3-34) activates the PKC pathway, whereas PTH (1-31) activates the PKA pathway. These data indicate that the PKC pathway plays a minor role in mediating the bone anabolic actions of PTH (Li *et al.*, 2007a).

Interestingly, Li and co-workers found in the same study that not only continuous PTH treatment led to higher expression levels of *Rankl*, but also intermittent administration. Intermittent PTH treatment led to a striking, but transient, increase in *Rankl* expression, whereas *Rankl* expression was moderately upregulated, but in a persistent manner, after continuous treatment. The authors suggest that the bone anabolic effect may be

accomplished by a short termed, increased bone resorption and a subsequent increased bone formation (Li *et al.*, 2007a).

Intermittent administration of PTH rapidly increases the expression of *Mcp1* in osteoblasts and therefore enhances osteoclast activity (Li *et al.*, 2007b). Recently, it was shown that the bone anabolic response after treatment with intermittent PTH is blocked in MCP1-KO mice (Tamasi *et al.*, 2013). These data indicate that the osteoclast regulating factor MCP1 is an important mediator for the bone anabolic effect of PTH.

Role of EGFR signaling in mediating the bone anabolic actions of PTH

There is accumulating evidence that the bone anabolic actions of intermittent PTH treatment are, at least in part, mediated via EGFR signaling. Two ligands of the EGFR, *Areg* and *Tgfa*, were identified as a PTH-regulated genes in rat UMR 106-01 osteoblastic cells. *Areg* expression was increased more than 2-fold after 4h and 12h of rat PTH (1-34) treatment (Qin *et al.*, 2003). Additional studies showed an increase in *Areg* mRNA levels in rat calvarial osteoblasts and mouse MC3T3 cells treated with rat PTH (1-34), as well as in the femurs of 4-week-old male rats after subcutaneous injections of human PTH (1-38), confirming that *Areg* is a PTH target gene *in vitro* and *in vivo* (Qin *et al.*, 2005). *In vitro*, administration of rat PTH (1-34) increased *Areg* expression levels 5-fold in the proliferative phase (day 6) and 23-fold in the mineralization phase (day 14) in rat calvarial osteoblasts, whereas the basal *Areg* expression levels did not change during the three phases of proliferation, differentiation and mineralization. *In vivo*, subcutaneous injections of human PTH (1-38) increased *Areg* expression 12-fold after 1h and 2-fold after 4h. Additional experiments revealed that *Areg* expression is also stimulated in rat primay osteoblastic cells after treatment with prostaglandin E_2 and 1,25-dihydroxyvitamin D_3, other osteotropic hormones that play important roles in bone remodeling (Qin *et al.*, 2005).

AREG stimulates proliferation and prevents differentiation and mineralization in rat calvarial osteoblasts. Addition of AREG to the medium significantly increased the number of cells and completely inhibited their mineralization (Qin *et al.*, 2005). In this study, the mRNA levels of bone markers, such as *Mmp13*, alkaline phosphatase, osteocalcin and osteonectin, were decreased in day 20 cultures. Western blot analysis revealed that

AREG treatment of osteoblastic cells stimulated the phosphorylation of AKT and ERK and increased the expression of *c-fos* and *c-jun* (Qin *et al.*, 2005).

Mice lacking AREG show no abnormalities in growth or body weight (Luetteke *et al.*, 1999). Microcomputed tomography (µ-CT) analysis of the tibial trabecular bone compartment of 4-week-old female AREG-KO mice revealed a significant reduction of trabecular number, trabecular thickness, connectivity density and percent bone volume, and consequently an increase in trabecular separation, whereas there were no differences in the femoral cortical bone compartment (Qin *et al.*, 2005), indicating that AREG plays a critical role in the development of trabecular bone. In line with these findings, recent studies of our group revealed a transient increase of trabecular bone mass in mice overexpressing *Areg* specifically in osteoblasts (Vaidya *et al.*, 2015).

Recently, AREG was identified as a chemotactic factor for mesenchymal progenitors. PTH-mediated release of AREG by osteoblastic cells promotes migration of mesenchymal progenitors *in vitro* via AKT and p38MAPK pathways. Conditioned media collected from cells with a siRNA knockdown of *Areg* do not possess this chemotactic activity (Zhu *et al.*, 2012).

In the latter study, Zhu and co-workers showed that the bone anabolic effect of intermittent PTH injections was blunted in $EGFR^{Wa5/flox}$ Col 3.6-Cre mice, which have a reduced EGFR activity in osteoblasts, indicating that the bone anabolic actions of PTH require EGFR signaling (Zhu *et al.*, 2012). In heterozygous Wa5 mice the bone anabolic effect of intermittent PTH treatment was fully maintained, most likely due to residual EGFR activity in these mice (Schneider *et al.*, 2012, Zhu *et al.*, 2012).

Aim of the study

In summary, AREG seems to be the major EGFR ligand mediating the bone anabolic actions of PTH. To clarify to which extent AREG is required for the bone anabolic effect of PTH, we treated 3-month-old female AREG-KO mice and controls intermittently with PTH or vehicle (saline) and examined their bone phenotype in detail.

3 Animals, Methods and Materials

Animals

AREG knockout (AREG-KO) mice were generated by Luetteke *et al.* (1999) and obtained from The Mutant Mouse Regional Resource Center (MMRRC) Repository at the University of North Carolina, USA. The AREG-KO mice were maintained in an inbred 129/C57BL/6 mixed background and housed under specified pathogen free conditions in a closed barrier facility with a 12 h light cycle at 25°C and 45% humidity. Health monitoring was performed according to FELASA (Federation of European Laboratory Animal Science Associations) recommendations. The mice were housed in Makrolon type II long and type III cages enriched with red houses and cellulose paper and had free access to standard rodent diet (V1534; Ssniff, Soest, Germany) and filtered tap water. The mice were weaned and marked with ear punches at the age of 4 weeks. Only females at an age of 3 months were used for the experiment.

All experiments were carried out in accordance with the German Animal Protection Law and authorized by the responsible veterinary authority.

Genotyping

For genotyping, ear punch tissues were collected in 1.5 ml vials (Eppendorf, Hamburg) and stored at -20 °C if not processed immediately. To isolate DNA, 620 µl digestion buffer were added to each tube and the samples were incubated overnight at 56 °C with gentle shaking.

Digestion buffer:	0.5 M EDTA pH 8.0	120 µl
	proteinase K (20 mg/ml in bidistilled H_2O)	17.5 µl
	Nuclei Lysis Solution	500 µl

After digestion, 3 µl RNAse (4mg/ml in bidistilled water) were added to each vial. The samples were incubated for 20 minutes at 37 °C to degrade RNA. Afterwards, to induce protein denaturation and precipitation, 200 µl protein precipitation solution were added and the samples were vortexed for 20 seconds at high speed and then chilled on ice for 5 minutes. The protein pellet was obtained via centrifugation (14 000 x g for 4

minutes) and the DNA containing supernatant was carefully transferred to a fresh vial containing 600 µl isopropanol to induce DNA precipitation. After gently inverting the tube for several times, the samples were centrifuged at 14 000 x g for 2 minutes. The supernatant was discarded. The remaining DNA pellet was washed in 600 µl 70% ethanol, and a pure pellet was obtained after centrifugation (14 000 x g for 2 minutes) and discarding the supernatant. The DNA pellet was air-dried for 10 to 15 minutes and rehydrated with 50 µl DNA Rehydration Solution. The DNA samples were stored at 4 °C.

Polymerase chain reaction (PCR) was performed using the Taq DNA polymerase Kit (Qiagen, Hilden). A mastermix was prepared on ice as follows (calculated per sample):

10x PCR reaction buffer (Qiagen, Hilden)	2.00 µl
dNTPs, 1 mM (MBI Fermentas, St. Leon-Rot)	2.00 µl
Q-Solution (Qiagen, Hilden)	4.00 µl
$MgCl_2$, 25mM (Qiagen, Hilden)	1.25 µl
Primer AregDel#1, 10 µM	1.00 µl
Primer AregDel#2, 10 µM	1.00 µl
Primer AregDel#3, 10 µM	1.00 µl
Bidistilled H_2O	6.65 µl
Taq Polymerase, 5 U/µl (Qiagen, Hilden)	0.10 µl
	∑ 19 µl

19 µl mastermix were added to each DNA template (1 µl) in a PCR-reaction tube.

Primer sequences:

AregDel#1: 5’ CTT TCC AGC TTT CTC CAC CTC AAG 3’

AregDel#2: 5’ ACA GTA ACC TCT GTT GCA TGC CAC 3’

AregDel#3: 5’ CTG CAC GAG ACT AGT GAG ACG TGC 3’

Thermal cycler conditions :

94°C - 5 minutes

94°C	-	45 seconds	36 x
59°C	-	45 seconds	
72°C	-	1 minute	
72°C	-	10 minutes	
4 °C	-	paused (till further process)	

The amplified products and molecular weight marker were loaded on a 1.5% agarose TAE gel containing ethidium bromide. Electrophoresis was carried out for 40 min at 120 Volt with TAE running buffer. The amplified DNA bands were visualized with ultra-violet light.

The primers AregDel#1 (sense) and AregDel#2 (antisense) both bind in the intron region before exon 3, leading to a ≈ 330 bp wild type allele signal. In AREG-KO mice, exons 3 and 4 are replaced by a neomycin cassette (Luetteke *et al.*, 1999). The primer AregDel#3 (antisense) binds to this cassette, leading to a ≈ 600 bp signal for the knock-out allele.

The 50x TAE stock contained:

TRIS	242 g
Glacial acetic acid	57.1 ml
0.5M EDTA pH 8.0	100 ml
ad 1000 ml bidistilled H_2O	

PTH treatment

3-month-old female AREG KO mice and WT controls received either 80µg/kg body weight (1-34) PTH (Bachem, Weil am Rhein, Germany) or vehicle (0.9% physiological saline solution) by subcutaneous injection once daily for five days per week over a period of four weeks. Additionally, all mice were subcutaneously injected with alizarin complexone (30 mg/kg body weight) once at the beginning of the experiment and with calcein (20 mg/kg body weight) on days 4 and 2 prior to necropsy.

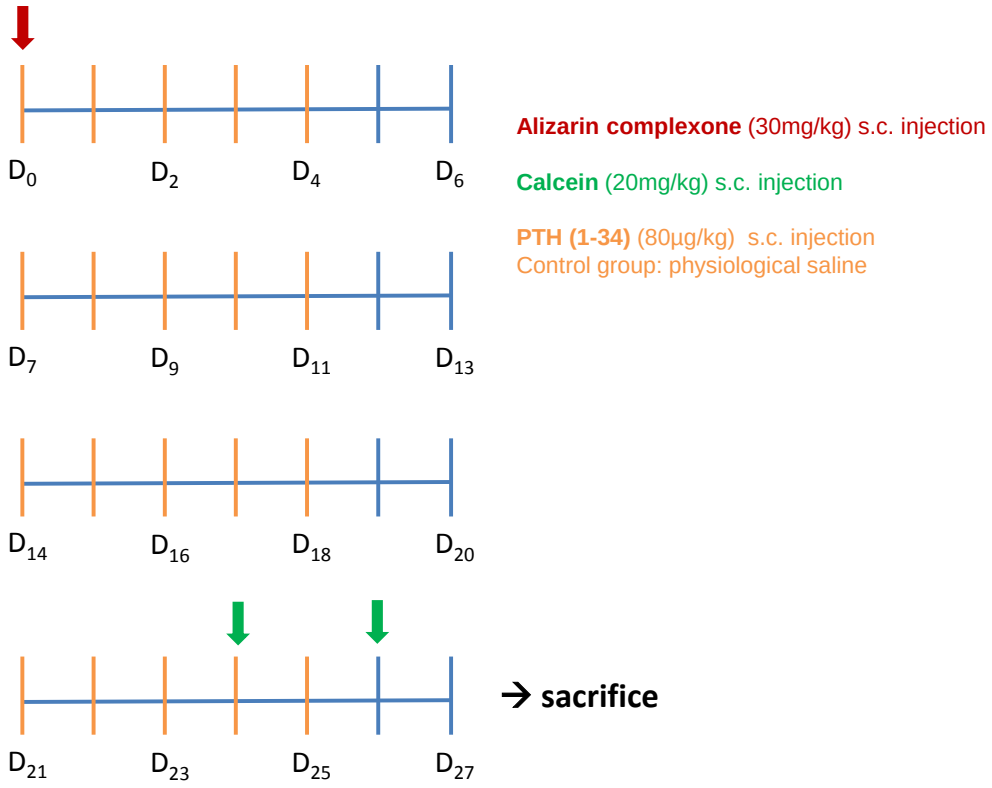

Figure 3 Schematic overview of the subcutaneous PTH and fluorochrome injections over the whole time of the experiment. AREG-KO and WT mice were subcutaneously injected with PTH (1-34) (80 mg/kg) or physiological saline five times a week for four weeks. Additionally, all animals received an injection with alizarine complexone (30 mg/kg) at the beginning of the experiment and calcein on days 4 and 2 before sacrifice.

Urine, serum and tissue collection

Spontaneous urine was collected and frozen at -20 °C until further analysis. Anesthetized mice were bled form the retrobulbar venous plexus with a heparinized capillary. To obtain serum, the blood samples were centrifuged for two times at 664 x g for 10 minutes in 1.5 ml centrifuge tubes and stored at -80°C until further analysis. The femurs and the first lumbar vertebrae (L1) were removed and cleaned.

Tissue preparation for histology and histomorphometry

Preparation of femurs and L1 for histology and histomorphometry was performed as described previously (Erben, 1997, Reim *et al.*, 2008, Schneider *et al.*, 2009a). First, the bones were fixed in 4% paraformaldehyde in PBS at 4 °C for 24h under gentle

shaking. Afterwards, the bones were washed with PBS for 24h at 4°C under gentle shaking.

The 10x PBS stock contained:

NaCl	80.0 g
Na_2HPO_4	14.4 g
KCl	2.0 g
KH_2PO_4	2.4 g

ad 1000 ml bidistilled H_2O

pH was adjusted to 7.4

After fixation and washing, the femurs and L1 were stored in 70% ethanol until further process. The right femur was cut in half using a precision band saw (Exakt, Norderstedt, Germany). The distal part of the femur and L1 were subsequently dehydrated and embedded in methylmethacrylate (MMA).

Dehydration:

Day 1:	96% ethanol
Day 2:	isopropanol
Day 8	xylene
Day 14:	MMA I
Day 18:	MMA II
Day 21:	MMA III
Day 25:	embedding

MMA I contained:

MMA	600 ml
Butylmethacrylate	50 ml
Methylbenzoate	50 ml
Polyethylglycol 400	12 ml

ad 1000 ml bidistilled H_2O

MMA II contained:

MMA	600 ml

Butylmethacrylate	50 ml
Methylbenzoate	50 ml
Polyethylglycol 400	12 ml
Benzylperoxide	4g
Ad 1000 ml bidistilled H_2O	

MMA III contained:

MMA	600 ml
Butylmethacrylate	50 ml
Methylbenzoate	50 ml
Polyethylglycol 400	12 ml
Benzylperoxide	8g
ad 1000 ml bidistilled H_2O	

For embedding, 4 ml/l N,N-Dimethyl-toluidine was added to MMA III to induce polymerization. The bones were embedded in 10 ml glass vials with a previously prepared plastic layer on the bottom. The vials were sealed with parafilm and transferred to a cooling chamber (-18 °C to -23 °C for 5 days).

After removing the glass vial and trimming the plastic block, 3-µm-tick sections of the femoral metaphysis and of the vertebral bodies were cut using a Microm HM360 microtome with a tungsten carbide knife. During cutting, the sections were kept wet with 0.1 % TWEEN® 20 and transferred carefully to APES-coated microscope slides.

For APES coating, the microscope slides were first incubated with aceton for 10 minutes and afterwards shortly rinsed with tap water. Thereafter, the slides were again incubated with aceton for 5 minutes and then incubated with APES solution, containing 4 ml APES in 200 ml Aceton. After APES coating, the slides were washed twice in bidistilled H_2O and incubated at 40°C-50°C overnight.

After transferring the sections to the APES-coated microscope slides, the sections were carefully stretched using 70 % ethanol, covered with polyethylene foil and pressed with a slide press for 3-4 days at 42 °C.

To obtain cross-sections of the femoral mid-diaphysis, the left femur was also embedded in MMA and 200-µm-sections were taken using a precision band saw. Subsequently, the sections were grounded to a final thickness of 20 µm using a micro-grinding system (Exakt Norderstedt, Germany). The sections were carefully glued on APES-covered microscopy slides.

Kossa/McNeal staining

To analyze bone formation, the longitudinal sections of the right femur and sections of the first lumbar vertebral bodies were stained with Kossa/McNeal tetrachrome according to standard protocols (Erben, 1997). The sections were deplastinized with methoxyethylacetat (for 60 minutes) and aceton (for 10 minutes) and washed with bidistilled H_2O (for 10 minutes). Next, the sections were incubated with 5% silver nitrate solution for 5-10 minutes (protected from light). After rinsing with bidistilled H_2O, the sections were incubated in a solution containing 5 % sodium carbonate and 9.25 % formaldehyde in bidistilled H_2O for 2 minutes. The sections were again rinsed with bidistilled H_2O and then incubated for 30 seconds in Farmer's Reducer. After rinsing under running tap water for 20 minutes and quickly washing with bidistilled H_2O, the sections were stained in a 5 % tetrachrome solution for 60 minutes. Thereafter, the slides were again rinsed in bidistilled H_2O and dehydrated with isopropanol and xylene. The slides were mounted with DePex (SERVA Electrophoresis GmbH, Heidelberg).

The Farmer's Reducer solution contained:

Sodium thiosulfate 10 %	200 ml
Potassium ferrocyanide 10 %	10 ml

The 5 % tetrachrome solution contained:

Methylene blue	0.5 g
Azur-A-Eosinat	0.8 g
Methylene violet	0.1 g
Methanol	250 ml
Glycerol	250 ml

Analysis of the osteoblast surface and the osteoid was performed using OsteoMeasure 3.0 (OsteoMetrics, Decatur, GA, USA) software, the DrawingBoard VI (GTCO CalComp, Scottsdale, AZ, USA) and the Axioskop 2 Plus (C. Zeiss, Jena, Germany). The area within 0.25 mm from the growth plates was excluded from the measurements.

Tartrate resistant alkaline phosphatase (TRAP) staining

To analyze bone resorption, the longitudinal sections of the right femur were stained for tartrate resistant alkaline phosphatase (TRAP) enzyme activity according to standard protocols (Erben, 1997, Schmidt *et al.*, 1999). The sections were deplastinized with methoxyethylacetat (for 60 minutes) and with aceton (for 10 minutes) and washed with bidistilled H_2O (for 10 minutes). Next, the sections were incubated in 0.2 M acetate buffer pH 5.0 for 20 minutes and afterwards with TRAP-reagent for 2-4 hours at 37°C. The slides were shortly rinsed with bidistilled H_2O, counterstained with Mayer's hematoxylin for 3 minutes and rinsed with tap water for 5-10 minutes. The stained sections were mounted with Kaiser's glycerol galantine (Merck, Darmstadt), an aqueous mounting medium.

The TRAP reagent contained:

naphtol AS-MX phosphate disodium salt	0.5 mg/ml
fast red TR salt	1,1 mg/ml
disolved in 0.2 M acetate buffer pH 5.0	

The hematoxylin staining solution contained:

Hematoxylin	1 g
Sodium iodide	0.2 g
Aluminium potassium sulfate	50 g
Chloral hydrate	50 g
Citric acid	1 g
Ad 1000 ml bidistilled H_2O	

Analysis of osteoclast numbers was performed using OsteoMeasure 3.0 (OsteoMetrics, Decatur, GA, USA) software, the DrawingBoard VI (GTCO CalComp, Scottsdale, AZ, USA) and the Axioskop 2 Plus (C. Zeiss, Jena, Germany). The area within 0.25 mm from the growth plates was excluded from the measurements.

Toluidine blue staining

Toluidine blue staining and automatic image analysis of cross-sections of the femoral mid-diaphysis were performed as described previously (Erben, 1997, Reim *et al.*, 2008, Weber *et al.*, 2004). First, the 20-µm undeplasticized microground sections were incubated with 30 % H_2O_2 under gentle shaking. After shortly rinsing the sections in tap water, the sections were stained in toluidine blue staining solution for 60 minutes.

The toluidine staining solution contained:

Toluidine blue O	2 g
Di-Sodium hydrogen phosphate	75 mg
Citric acid	158 mg
ad 100 ml bidistilled H_2O	

After staining and air-drying for 2 hours, the sections were mounted with DePex.

Automatic image analysis was performed using the AxioVision 4.6 (C. Zeiss, Jena, Germany) software.

Mounting with Fluoromount

To measure the cortical mineral apposition rate (MAR) and the trabecular bone formation rate (BFR), undeplasticized and unstained longitudinal sections of the distal femoral metaphysis, cross-sections of the femoral mid-diaphysis and sections of the first lumbar vertebral bodies were mounted with Fluoromount (Serva, Heidelberg, Germany) as described previously (Erben, 1997).

Analysis of the trabecular BFR and the cortical MAR was performed using OsteoMeasure 3.0 (OsteoMetrics, Decatur, GA, USA) software, the DrawingBoard VI (GTCO CalComp, Scottsdale, AZ, USA) and the Axioskop 2 Plus (C. Zeiss, Jena, Germany). The border of the trabecular and cortical bone were traced under blue violet excitation (395-440 nm) and the calcein and alizarin complexone labels were traced under blue excitation (450-490 nm) to reduce background. In the distal femoral metaphysis and in L1, the area within 0.25 mm from the growth plates was excluded from the measurements.

Biochemical bone markers

Analysis of biochemical bone markers was kindly conducted by Claudia Bergow from the laboratory of Prof. Reinhold Erben, Vienna, Austria. Serum osteocalcin levels were measured with an immunoradiometric assay (Mouse Osteocalcin ELISA kit, Immutopics International) according to the manufacturer's instructions. Total collagen cross-link deoxypyridinoline was measured with the MicroVue DPD EIA kit (Quidel Corporation, USA) according to the manufacturer's instructions and normalized to urinary creatinine levels, measured with a Cobas c111 autoanalyzer (Roche Diagnostics).

Statistical analyses

Statistical analyses were performed using the SPSS software for Windows 17.0 (SPSS Inc., Chicago, USA). Differences between the groups were analyzed by one-way ANOVA followed by Student-Newman-Keuls (SNK) test as *post hoc* test. Additionally, the data were analyzed by two-way ANOVA to evaluate the individual effects of PTH treatment and the knocked out *Areg* gene, as well as their 2-way interaction. The graphs were generated with GraphPad Prism 5.0 (GraphPad Software Inc., La Jolla, USA). *P* values lower than 0.05 were considered significant. The data are presented as means ± SEM.

Materials

Machines and software

Agarose gel electrophoresis chamber	MWG-Biotech, Ebersberg, Germany
Axioskop 2 Plus	C. Zeiss, Jena, Germany
AxioVision 4.6	C. Zeiss, Jena, Germany
Band Saw	EXAKT Apparatebau GmbH, Norderstedt, Germany
Centrifuge (5417R)	Eppendorf, Hamburg, Germany
Cobas c111 autoanalyzer	Roche Diagnostics, Germany
GraphPad Prism 5.0	GraphPad Software Inc., La Jolla, USA

Incubator	Thermo Fisher Scientific, Schwerte, Germany
Microgrinding System	EXAKT Apparatebau GmbH, Norderstedt, Germany
Micrometer	Mitutoyo Deutschland GmbH, Ingolstadt, Germany
Microtome HM 360	Microm International GmbH, Waldorf, Germany
Microwave	Siemens, München, Germany
MS1 Minishaker	IKA process equipment, Staufen
OsteoMeasure 3.0	OsteoMetrics, Decatur, GA, USA
SPSS	SPSS Inc., Chicago, USA
Thermocycler	Biometra®, Göttingen, Germany
Thermomixer	Eppendorf, Hamburg, Germany
Wise Shake® Shaker, SHR-1D	Wisd Laboratory Instruments, Laboratory Supplies Ltd., Dublin, Ireland

Consumables

Filter paper circles, Ø 150 mm	Whatman GmbH, Dassel, Germany
Glass microscope slides	Menzel-Gläser, Braunschweig, Germany
Grinding disks	Hermes Schleifmittel, Hamburg, Germany
Microscope cover glasses, 24 x 50 mm	VWR International, Darmstadt, Germany
Microscope cover glasses, 18 x 18 mm	VWR International, Darmstadt, Germany
Parafilm	VWR International, Darmstadt, Germany
Pasteur pipette, 5 ml	VWR International, Darmstadt, Germany
Pasteur pipette, 7 ml	VWR International, Darmstadt, Germany

Polyethylene foil	Heraeus Kulzer GmbH, Hanau, Germany
QualiPCRTube-strips	Kisher Biotech, Steinfurt, Germany
Safe-lock tubes, 1.5 ml	Eppendorf, Hamburg, Germany
Standard rodent diet (V1534)	Ssniff, Soest, Germany
Tungsten carbide knife	Microm International GmbH, Waldorf, Germany

Chemicals

Agarose	Invitrogen, Karlsruhe, Germany
Alizarine complexone	Sigma-Aldrich, Schnelldorf, Germany
APES (Aminopropyltriethoxysilane)	Sigma-Aldrich, Deisenhofen, Germany
Azur-A-Eosin	Merck, Darmstadt, Germany
Benzylperoxide	Merck, Darmstadt, Germany
Butylmethacrylate	Sigma-Aldrich, Deisenhofen, Germany
Calcein	Sigma-Aldrich, Schnelldorf, Germany
DePex	SERVA Electrophoresis GmbH, Heidelberg, Germany
DNA Rehydration Solution	Promega, Mannheim, Germany
dNTPs	Thermo Scientific, St. Leon-Roth, Germany
EDTA	VWR, Darmstadt, Germany
Ethanol	Carl Roth, Karlsruhe, Germany
Ethidiumbromide	Carl Roth GmbH, Karlsruhe, Germany
Fast Red TR	Sigma-Aldrich, Deisenhofen, Germany
Fluoromount	SERVA Electrophoresis GmbH, Heidelberg, Germany
Formaldehyde Solution, 37 %	Merck, Darmstadt, Germany
Gene Ruler, 100 bp	Thermo Scientific, St. Leon-Roth, Germany
Glacial acetic acid	Carl Roth, Karlsruhe, Germany
Glycerol	Merck Schuchardt, Hohenbrunn, Germany

Hematoxylin	Merck, Darmstadt, Germany
Hydrogen peroxide, 30 %	Merck Schuchardt, Hohenbrunn, Germany
Isopropanol	VWR, Darmstadt, Germany
Kaiser's glycerol gelantine	Merck, Darmstadt, Germany
KCl	Merck, Darmstadt, Germany
KH_2PO_4	Merck, Darmstadt, Germany
Loctite ® 420 glue	Henkel AG & Co. KGaA, Düsseldorf, Germany
Methoxyethyl acetate	Merck, Darmstadt, Germany
Methyl alcohol	Sigma-Aldrich, Deisenhofen, Germany
Methylbenzoate	Merck, Darmstadt, Germany
Methylene blue	Merck, Darmstadt, Germany
Methylene violet	Chroma-Gesellschaft Schmid & Co., Stuttgart-Untertürkheim, Germany
Methylmethacrylate	Merck, Darmstadt, Germany
MicroVue DPD EIA kit	Quidel Corporation, USA
Mouse Osteocalcin ELISA kit	Immutopics International, USA
Na_2HPO_4	Merck, Darmstadt, Germany
Naphtol AS-MX phosphate	Sigma-Aldrich, Deisenhofen, Germany
N,N-Dimethyl-toluidine	Merck, Darmstadt, Germany
Nuclei Lysis Solution	Promega, Mannheim, Germany
Paraformaldehyde	Sigma-Aldrich, Deisenhofen, Germany
Polyethylglycol	Merck, Darmstadt, Germany
Potassium ferrocyanide	Sigma-Aldrich, Deisenhofen, Germany
Protein Precipitation Solution	Promega, Mannheim, Germany
Proteinase K, 20 mg/ml	Roche, Mannheim, Germany
PTH	Bachem, Weil am Rhein, Germany
RNAse	Promega, Mannheim, Germany
Silver nitrate	Merck, Darmstadt, Germany
Sodium acetate	Merck, Darmstadt, Germany
Sodium carbonate	Merck, Darmstadt, Germany
Sodium iodide	Sigma-Aldrich, Deisenhofen, Germany
Sodium thiosulfate pentahydrate , 10%	Merck, Darmstadt, Germany

Taq DNA Polymerase Kit	Qiagen, Hilden, Germany
Tartratic acid	Merck, Darmstadt, Germany
TRIS	Carl Roth, Karlsruhe, Germany
TWEEN ® 20	Sigma-Aldrich, Deisenhofen, Germany
Xylene	Herba Chemosan Apotheker AG, Wien, Austria

4 Results

Cortical bone histomorphometry of the femoral shaft

Analysis of cross-sections of the femoral mid-diaphysis revealed a profound increase of periosteal and endocortical bone in the PTH-treated AREG-KO and WT mice as compared to their saline-treated controls, as shown by the red alizarine complexone line given at the start of the experiment. Measurement of the periosteal and endocortical mineral apposition rate (MAR) confirmed these findings. Both the periosteal and the endocortical MAR were significantly increased in PTH-treated AREG-KO and WT mice as compared to their controls.

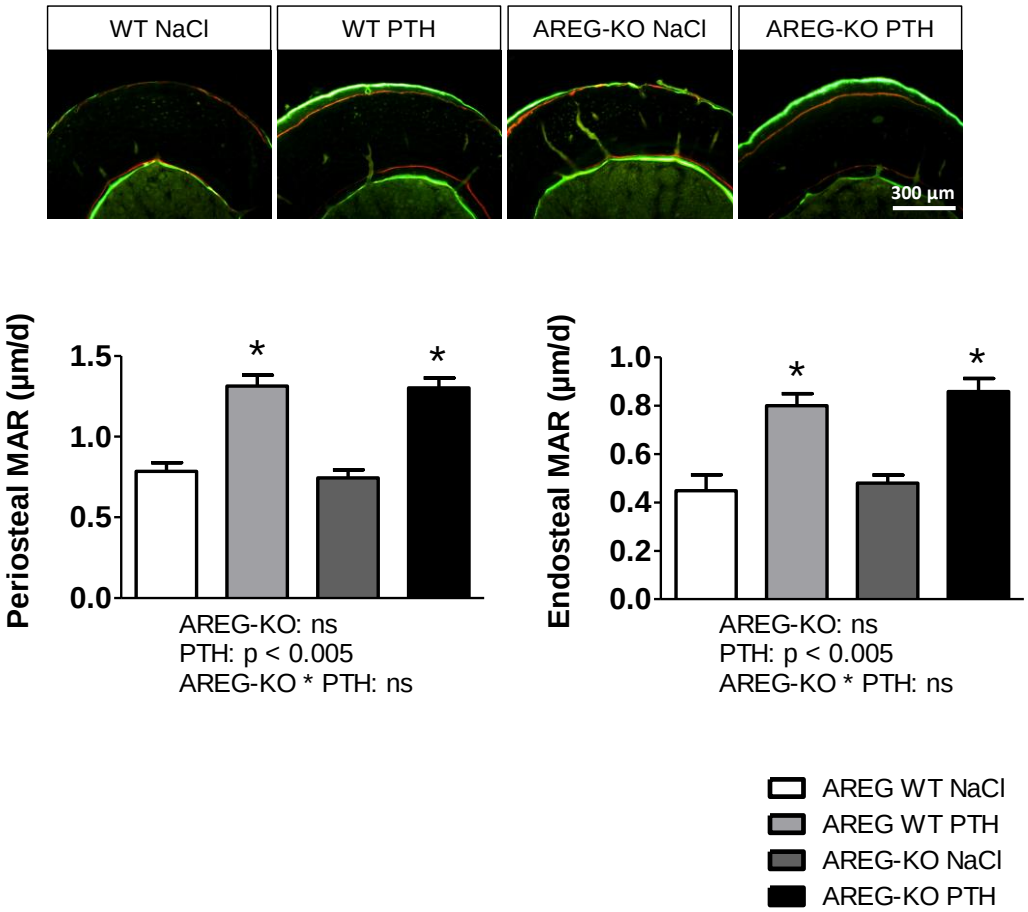

Figure 4 Fluorochrome labeling showing the newly formed cortical bone over the whole 4-week experimental period as shown by the red alizarin complexone line. Graphs show the periosteal and the endocortical mineral apposition rate (MAR). Data are means ± SEM of 13-14 animals/group. * denotes $p < 0.05$ vs. the respective vehicle-treated group. Results of 2-way ANOVA are shown below the graphs.

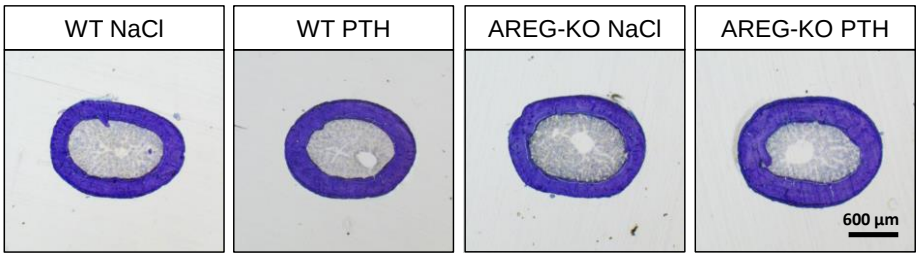

Figure 5 Toluidine blue-stained histological pictures of 20-µm microground cross-sections of the femoral midshaft showing an increase of cortical bone in the PTH-treated AREG-KO and WT mice as compared to their saline-treated controls.

Toluidine blue-stained histological sections of the femoral midshaft also showed an increase of cortical bone in the PTH-treated AREG-KO and WT mice as compared to their control groups. However, automatic image analysis of toluidine blue-stained 20-µm-thick microground sections of the femoral midshaft showed only mild changes. The cortical area (Ct.Ar) and the cortical thickness (Ct.Th) were increased in PTH-treated WT mice as compared to their saline-treated controls, whereas the total (cross-sectional) area (TtCross-sectAr), the marrow area (Ma.Ar) and its relation to the total area, the intracortical pore area (hole area, HoleAr) and its relation to the total area, the intracortical pore number (hole number, HoleNo), the pore perimeter (hole perimeter, HolePm), the cortical area (Ct.Ar) in its relation to the total area (Ct.Ar/Tt.Ar.), the bone perimeter (B.Pm), the periosteal (Ps.BPm) and endocortical bone perimeter (Ec.BPm) were unchanged between the groups as shown in Figures 6a and 6b. No differences were seen between saline-treated WT and AREG-KO mice.

In conclusion, the bone anabolic effect of intermittent PTH treatment was fully maintained in the femoral cortical bone of AREG-KO mice.

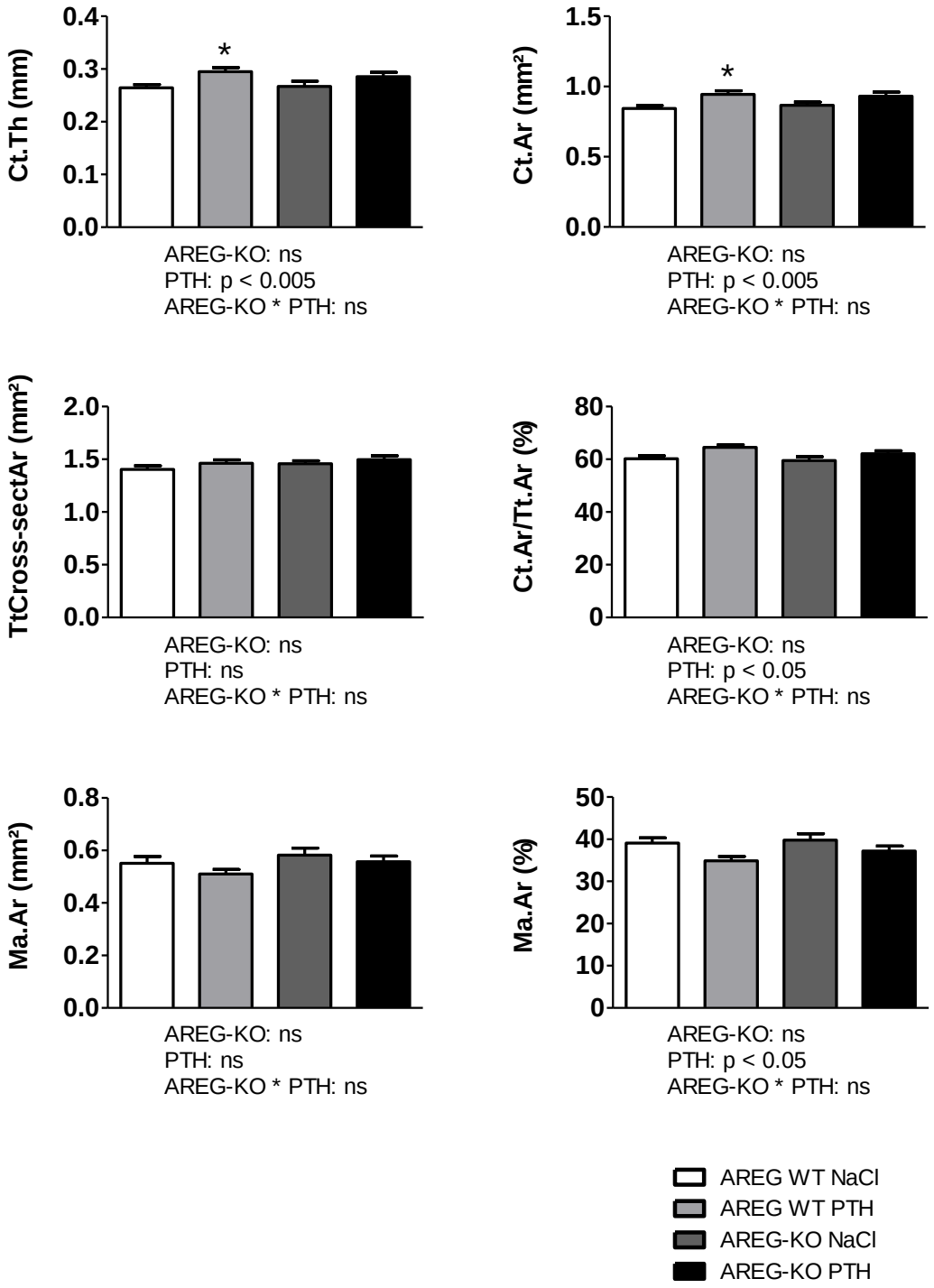

Figure 6a Automatic image analysis of toluidine blue-stained 20-µm microground cross-sections of the femoral midshaft. The cortical thickness (Ct.Th) and area (Ct.Ar) were increased in WT mice after four weeks of PTH treatment as compared to their saline-treated controls. The cortical area in relation to the total area (Ct.Ar/Tt.Ar) remained unchanged. No differences were found in total cross-sectional area (TtCross-sectAr), marrow area (Ma.Ar) and its relation to the total area. Data are means ± SEM of 9-10 animals/group. * denotes $p < 0.05$ vs. the respective vehicle-treated group. Results of 2-way ANOVA are shown below the graphs.

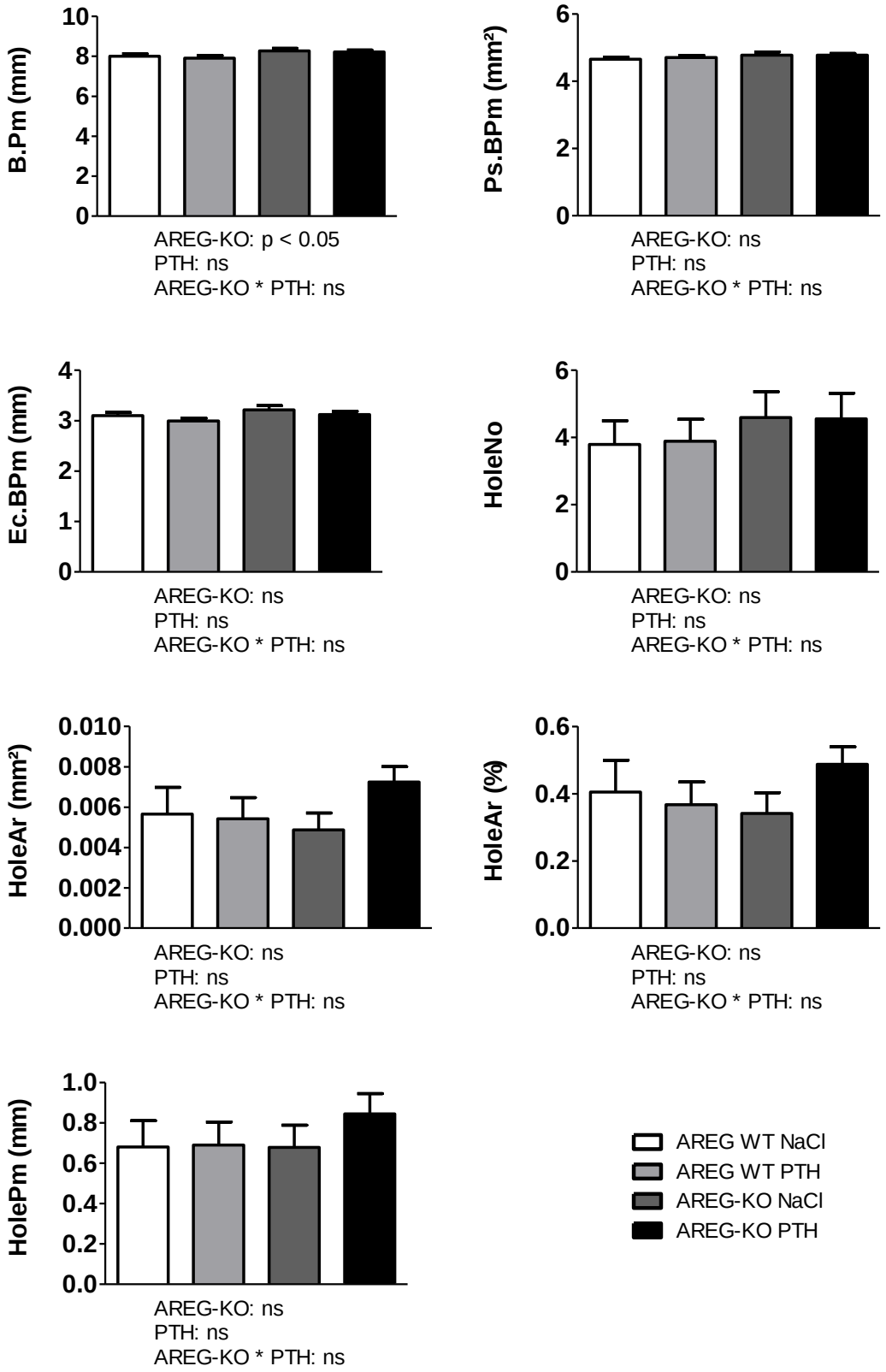

Figure 6b Automatic image analysis of toluidine blue-stained 20-µm microground cross-sections of the femoral midshaft. No differences between the groups were found in bone perimeter (B.Pm), the periosteal (Ps.BPm) and endocortical bone perimeter (Ec.BPm), the intracortical pore area (hole area, HoleAr) and in its relation to the total area, in the number of intracortical pores (hole number, HoleNo) or their perimeter (HolePm). Data are means ± SEM of 9-10 animals/group. * denotes $p < 0.05$ vs. the respective vehicle-treated group. Results of 2-way ANOVA are shown below the graphs.

Cancellous bone histomorphometry of the distal femoral metaphysis

Histology of Kossa/McNeil-stained longitudinal sections of the distal femoral metaphysis revealed a profound increase of cortical and cancellous bone in both PTH-treated groups as compared to their saline-treated controls.

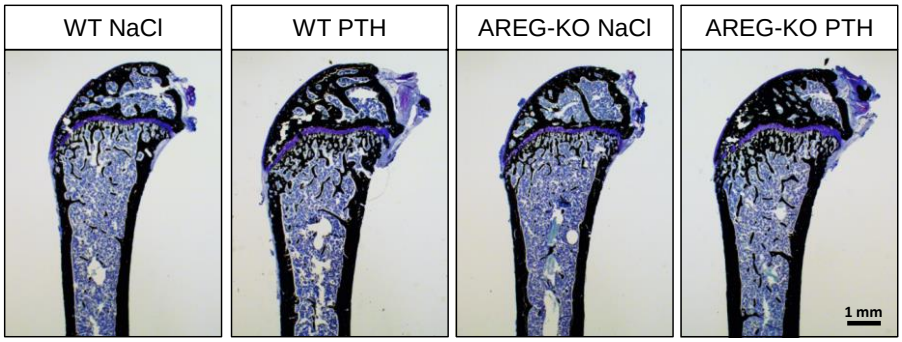

Figure 7 Kossa/McNeil-stained longitudinal sections of the distal femur showing an increase of bone mass in the PTH-treated WT and AREG-KO mice as compared to their saline-treated controls.

Analysis of Kossa/McNeil-stained sections of the distal femoral metaphysis showed that the osteoblast surface (in relation to the bone surface, Ob.S/BS), the osteoid surface (in relation to the bone surface, OS/BS) and the osteoid volume (in relation to the bone volume, OV/BV) were unchanged between the groups. The osteoid thickness (O.Th) was increased in PTH-treated WT mice as compared to their saline-treated controls and the same tendency was seen in PTH-treated AREG-KO animals as compared to their controls as shown in Figure 8.

The mineral apposition rate (MAR) and the bone formation rate (BFR) were increased in both PTH-treated groups as compared to their vehicle-treated controls as shown in Figure 9. The amount of newly formed trabecular bone was measured by the distance between the two green calcein labels. No significant differences were found between saline-treated AREG-KO and WT mice and PTH-treated AREG-KO and WT mice.

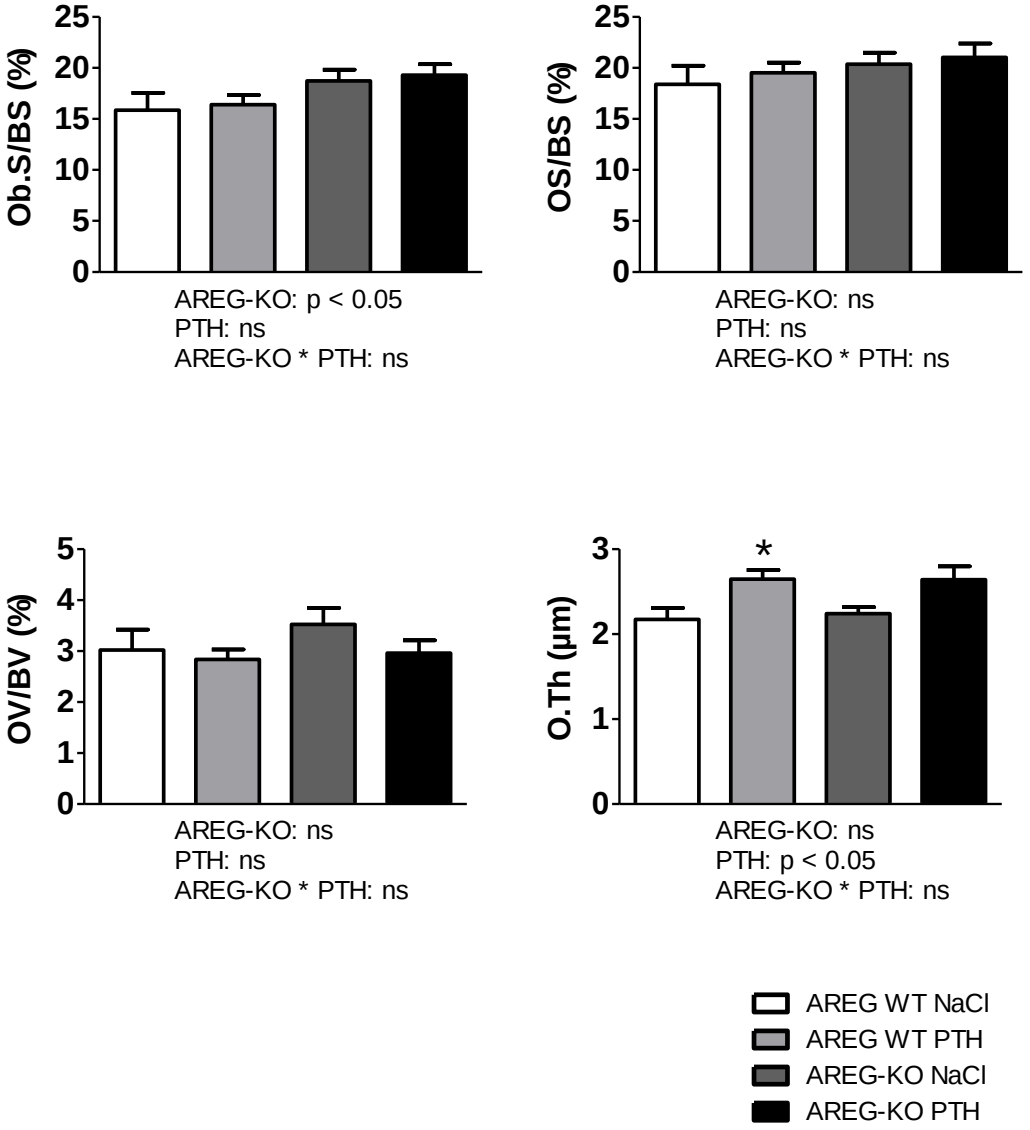

Figure 8 Analysis of Kossa/McNeil-stained longitudinal sections of the distal femur showing no differences in Ob.S./BS (osteoblast surface in relation to bone surface), in OS/BS (osteoid surface in relation to bone surface) and OV/BV (osteoid volume in relation to bone volume). The osteoid thickness (O.Th) was increased in PTH-treated WT mice as compared to their saline-treated controls. Data are means ± SEM of 13-14 animals/group. * denotes $p < 0.05$ vs. the respective vehicle-treated group. Results of 2-way ANOVA are shown below the graphs.

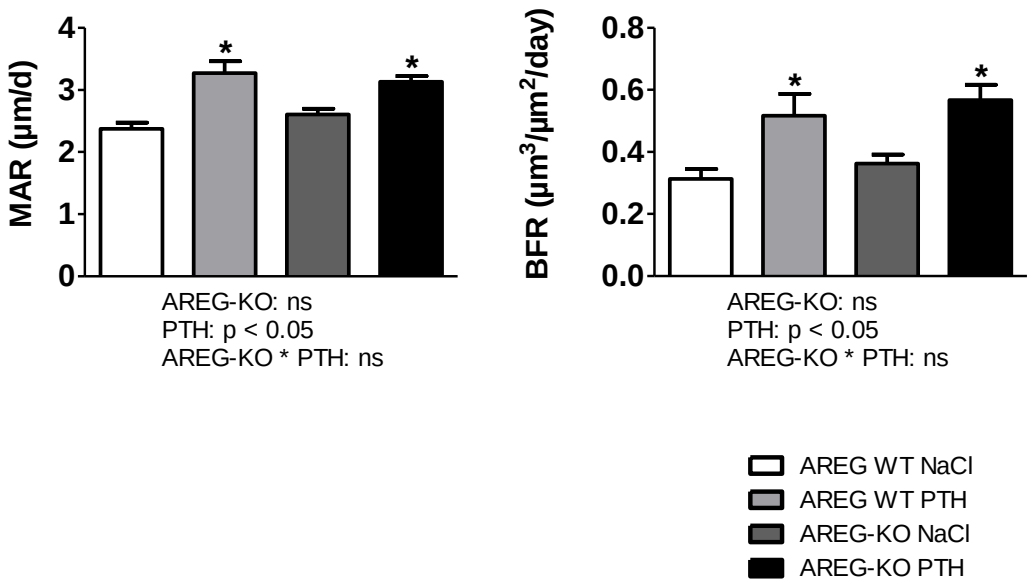

Figure 9 Mineral apposition rate (MAR) and bone formation rate (BFR) were increased in the distal femoral metaphysis in PTH-treated WT and AREG-KO mice as compared to their saline-treated controls. Data are means ± SEM of 13-14 animals/group. * denotes $p < 0.05$ vs. the respective vehicle-treated group. Results of 2-way ANOVA are shown below the graphs.

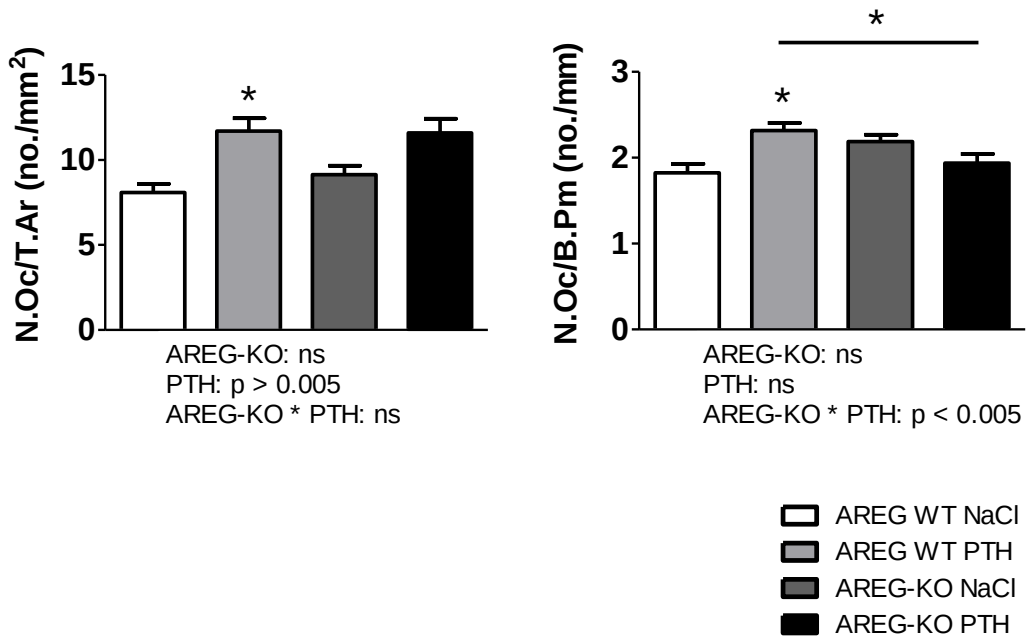

Figure 10 Analysis of TRAP-stained longitudinal cross-sections of the femoral metaphysis to analyze bone resorption showing an increased number of osteoclasts per tissue area (N.Oc/T.Ar) and per bone perimeter (N.Oc/B.Pm) in PTH-treated WT mice as compared to their saline-treated controls. The number of osteoclasts per bone perimeter (N.Oc/B.Pm) was significantly lower in PTH-treated AREG-KO mice as compared to PTH-treated WT mice. Data are means ± SEM of 14 animals/group. * denotes $p < 0.05$ vs. the respective vehicle-treated group unless stated otherwise. Results of 2-way ANOVA are shown below the graphs.

Analysis of TRAP-stained sections of the femoral metaphysis revealed an increased number of osteoclasts per tissue area (N.Oc/T.Ar) in PTH-treated WT mice as compared to saline-treated WT mice. The same tendency was seen in PTH-treated AREG-KO mice as compared to their saline-treated controls. Interestingly, the number of osteoclasts per bone perimeter (N.Oc/B.Pm) was increased in PTH-treated WT mice as compared to their saline-treated controls, whereas no such tendency was seen in the PTH- and vehicle-treated AREG-KO mice. On the contrary, the number of osteoclasts per bone perimeter was significantly decreased in PTH-treated AREG-KO mice in comparison to their WT control as shown in Figure 10.

Automatic image analysis of Kossa/McNeil-stained sections of the distal femoral metaphysis revealed an PTH-mediated increase in the trabecular area (Tb.Ar), the bone area in its relation to the tissue area (B.Ar/T.Ar), the bone perimeter in its relation to the tissue area (B.Pm/T.Ar), the trabecular number (Tb.N), the trabecular width (Tb.Wi) and the bone surface in relation to the tissue volume (BS/TV) in both PTH-treated WT and AREG-KO mice as compared to their vehicle-treated controls. Because of the increased number of trabeculae and their increased area and width, the trabecular separation was decreased in PTH-treated WT and AREG-KO mice in comparison to their saline-treated controls. The trabecular number per bone area (N.Tb/B.Ar) was decreased in PTH-treated WT and AREG-KO mice as compared to their saline-treated controls. The number of trabeculae in relation to the tissue area (N.Tb/T.Ar) was decreased in PTH-treated WT mice as compared to their vehicle-treated control. The results of the automatic image analysis of the femoral metaphysis are shown in Figures 11a and 11b.

In summary, absence of AREG did not alter the effects of intermittent PTH treatment. The bone anabolic effect was maintained in the femoral trabecular bone compartment of AREG-KO mice. However, the number of osteoclasts per bone perimeter (N.Oc/B.Pm) was decreased in PTH-treated AREG-KO mice as compared to their WT control, indicating a decreased osteoclast formation under PTH-mediated bone anabolic conditions in AREG-KO mice.

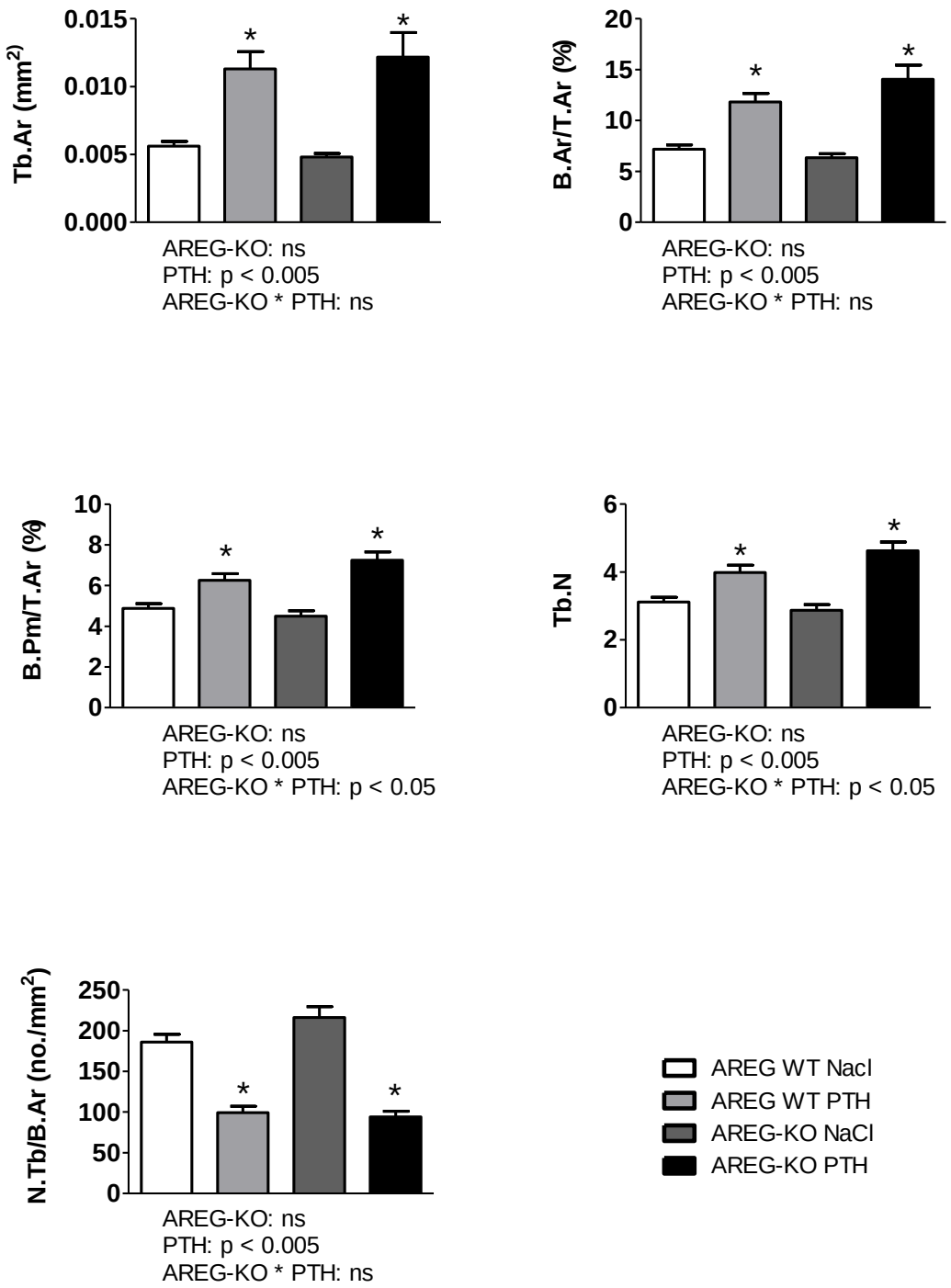

Figure 11a Automatic image analysis of Kossa/McNeil-stained longitudinal cross-sections of the distal femoral metaphysis showing an increase in the trabecular area (Tb.Ar), the bone area in its relation to the tissue area (B.Ar/T.Ar), the bone perimeter in its relation to the tissue area (B.Pm/T.Ar) and the trabecular number (Tb.N) in PTH-treated WT and AREG-KO mice as compared to their saline-treated controls. The number of trabeculae per bone area (N.Tb/B.Ar) was decreased in PTH-treated WT and AREG-KO mice in comparison to their saline-treated controls. Data are means ± SEM of 13-14 animals/group. * denotes $p < 0.05$ vs. the respective vehicle-treated group. Results of 2-way ANOVA are shown below the graphs.

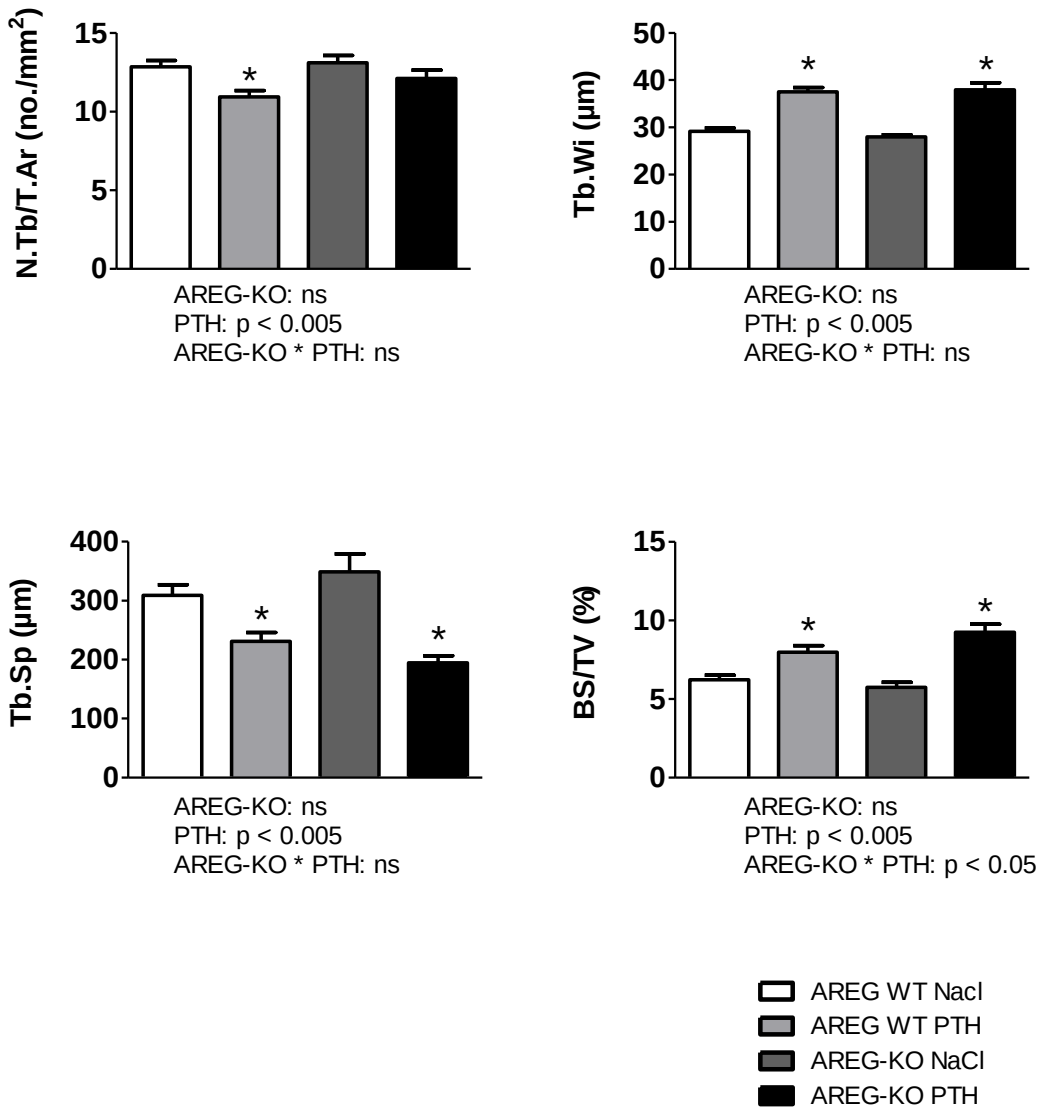

Figure 11b Automatic image analysis of Kossa/McNeil-stained longitudinal cross-sections of the distal femoral metaphysis showing a decreased number of trabeculae in relation to the tissue area (N.Tb/T.Ar) in PTH-treated WT mice as compared to their saline-treated controls. The trabecular width (Tb.Wi) was increased in both PTH-treated WT and AREG-KO mice as compared to their saline-treated controls, and vice versa, the trabecular separation (Tb.Sp) was decreased. The relation of the bone surface to the tissue volume (BS/TV) was increased in PTH-treated WT and AREG-KO mice in comparison to their saline-treated controls. Data are means ± SEM of 13-14 animals/group. * denotes $p < 0.05$ vs. the respective vehicle-treated group. Results of 2-way ANOVA are shown below the graphs.

Cancellous bone histomorphometry of the first lumbar vertebra

The amount of newly formed trabecular bone was measured by the distance of the two green calcein labels under fluorescent light in midsagittal sections of first lumbar (L1) vertebral bodies. The mineral apposition rate (MAR) was increased in PTH-treated WT mice in comparison to their vehicle-treated control, whereas there were only mild changes in the PTH-treated AREG-KO mice as compared to their controls. In line with the findings in the trabecular bone compartment of the distal femoral metaphysis, the bone formation rate (BFR) was increased after intermittent PTH treatment in both WT and AREG-KO mice as compared to their saline-treated controls as shown in Figure 12.

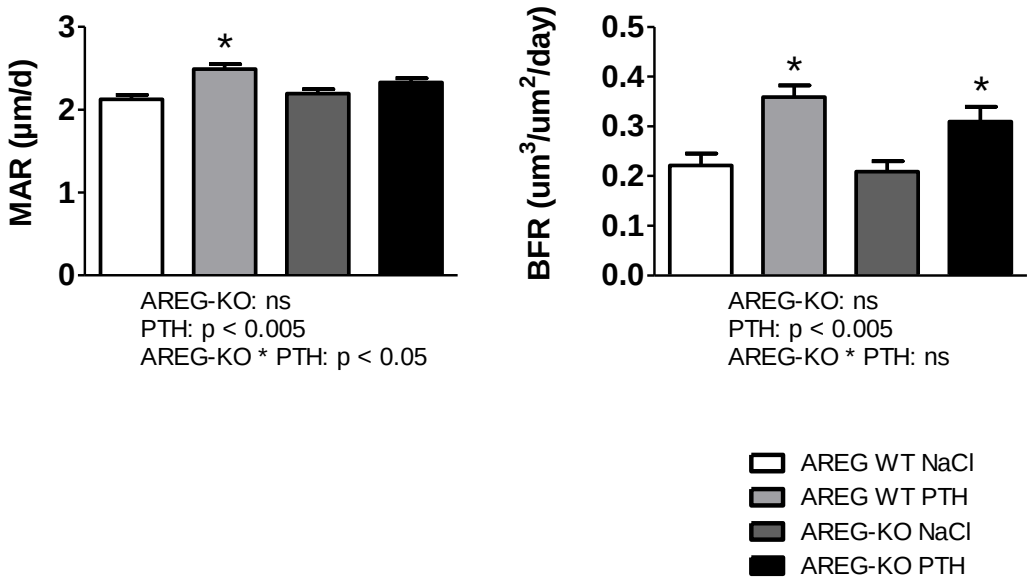

Figure 12 Mineral apposition rate (MAR) and bone formation rate (BFR) of the trabecular bone in the first lumbar vertebra. The MAR was increased in PTH-treated WT mice as compared to their saline-treated controls. The BFR was increased in both PTH-treated WT and AREG-KO mice as compared to their controls. Data are means ± SEM of 14 animals/group. * denotes $p < 0.05$ vs. the respective vehicle-treated group. Results of 2-way ANOVA are shown below the graphs.

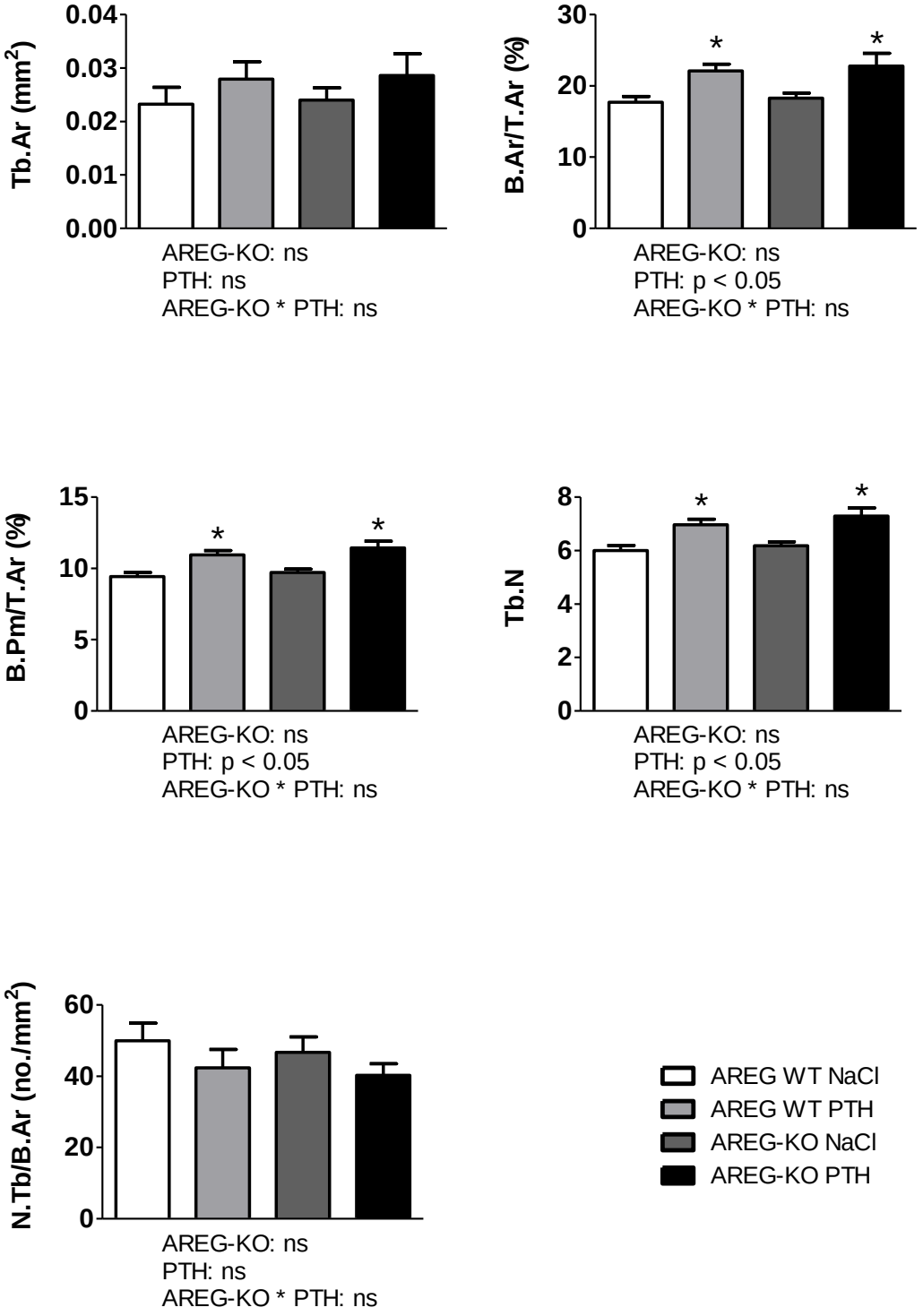

Figure 13a Automatic image analysis of Kossa/McNeil-stained first lumbar vertebral bodies showing an increase of the bone area in its relation to the tissue area (B.Ar/T.Ar), the bone perimeter in its relation to the tissue area (B.Pm/T.Ar) and the trabecular number (Tb.N) in PTH-treated WT and AREG-KO mice as compared to their saline-treated controls. No significant differences were seen in the trabecular area (Tb.Ar) and the number of trabeculae in relation to the bone area (N.Tb/B.Ar). Data are means ± SEM of 13-14 animals/group. * denotes $p < 0.05$ vs. the respective vehicle-treated group. Results of 2-way ANOVA are shown below the graphs.

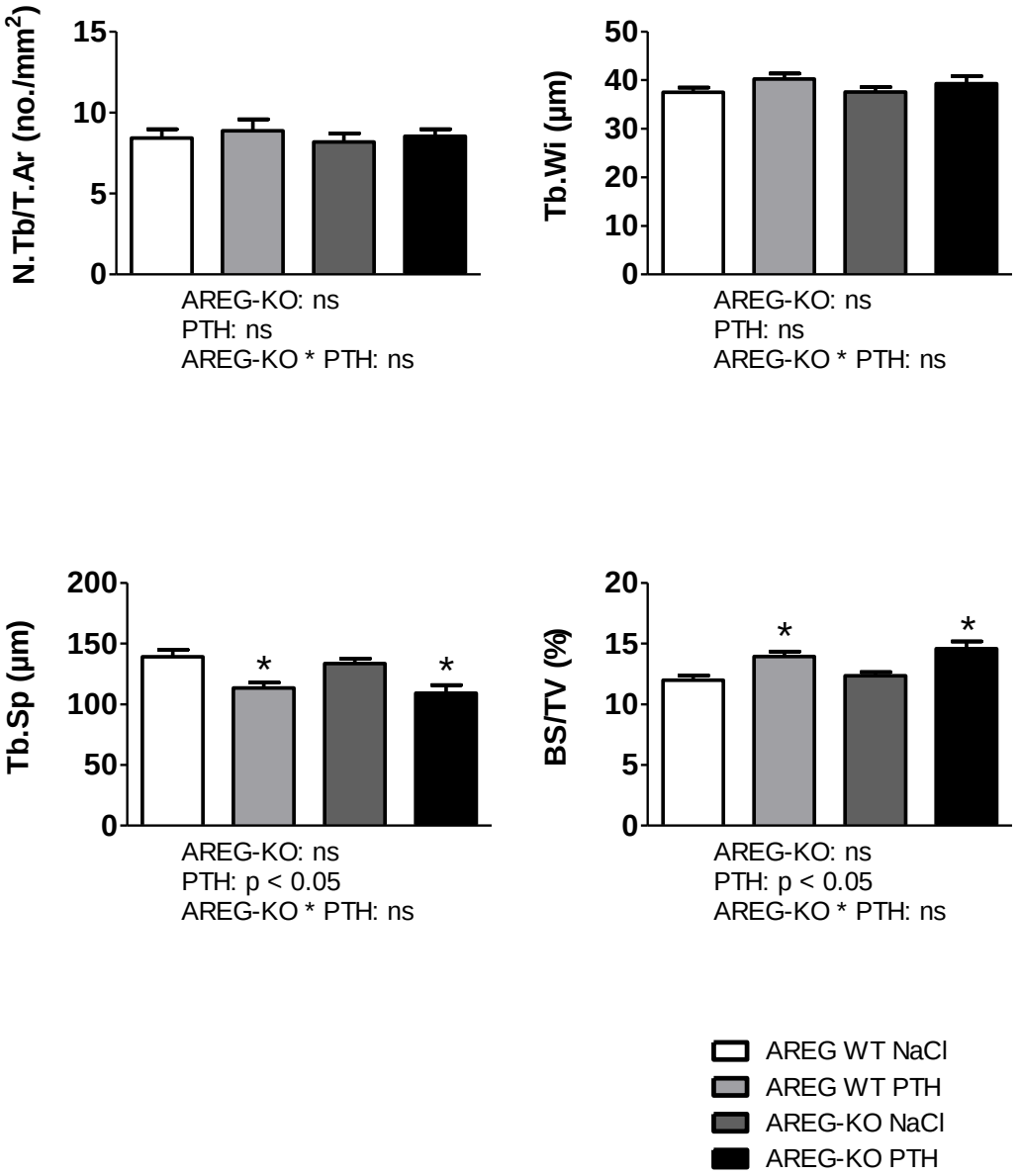

Figure 13b Automatic image analysis of Kossa/McNeil-stained first lumbar vertebral bodies showing an increase in the bone surface in its relation to the tissue volume (BS/TV) in both PTH-treated WT and AREG-KO mice as compared to their saline-treated controls. No significant differences were seen in the number of trabeculae in relation to the tissue area (N.Tb/T.Ar) and the trabecular width (Tb.Wi). The trabecular separation (Tb.Sp) was decreased in PTH-treated WT and AREG-KO mice as compared to their controls. Data are means ± SEM of 13-14 animals/group. * denotes $p < 0.05$ vs. the respective vehicle-treated group. Results of 2-way ANOVA are shown below the graphs.

Automatic image analysis of Kossa/McNeil-stained sections of the first lumbar vertebral bodies revealed an increase in the bone area in its relation to the tissue area (B.Ar/T.Ar), the bone perimeter in its relation to the tissue area (B.Pm/T.Ar), the trabecular number (Tb.N) and the bone surface in relation to the tissue volume (BS/TV) in both PTH-treated WT and AREG-KO mice as compared to their saline-treated controls as shown in Figures 13a and 13b. These findings were in line with the previous results of the trabecular bone compartment in the distal femoral metaphysis. The trabecular separation (Tb.Sp) was decreased in both PTH-treated groups as compared to their vehicle-treated controls. The trabecular area (Tb.Ar), the number of trabeculae in its relation to the bone area (N.Tb/B.Ar), the number of trabeculae in relation to the tissue area (N.Tb/T.Ar) and the trabecular width (Tb.Wi) remained unaffected by intermittent PTH treatment in both WT and AREG-KO mice.

Analysis of serum Osteocalcin and urinary deoxypyridinoline

To evaluate the effect of intermittent PTH treatment at the whole body level, the serum level of osteocalcin, a systemic marker for bone formation, and the excretion of urinary collagen crosslink deoxypyridinoline (DPD), a marker for bone resorption, were measured by ELISA.

Serum osteocalcin was increased in PTH-treated WT and AREG-KO mice as compared to their vehicle-treated controls as shown in Figure 14. These findings were in line with the increased BFR in the trabecular and cortical bone compartment, further suggesting that intermittent PTH treatment might lead to an increased bone anabolism at the whole body level in both WT and AREG-KO mice and that this effect might not only be restricted to the femur and the first lumbar vertebra, but also present at the whole body level.

The level of urinary DPD remained unchanged by intermittent PTH treatment in WT and AREG-KO mice, indicating that the possible effect of intermittent PTH treatment on bone resorption could not be assessed with this marker. The results of urinary DPD levels are shown in Figure 14.

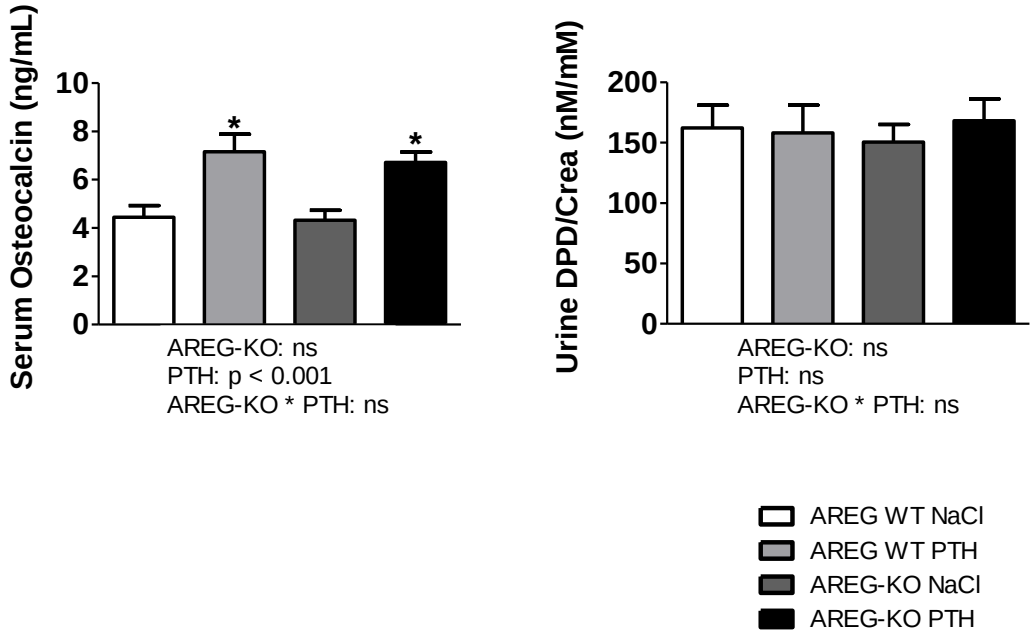

Figure 14 Serum osteocalcin and urinary deoxypyridinoline/creatinine (DPD/Crea) levels in vehicle and PTH-treated WT and AREG-KO mice after 4 weeks of intermittent PTH treatment. Serum osteocalcin was increased in both PTH-treated WT and AREG-KO mice as compared to their saline-treated controls, whereas urine DPD remained unchanged. Data are means ± SEM of 12-14 animals/group. * denotes $p < 0.05$ vs. the respective vehicle-treated group by 1-way ANOVA followed by SNK test. Results of 2-way ANOVA are shown below the graphs.

5 Discussion

To investigate to which extent AREG is required for the bone anabolic actions of PTH, we treated AREG-KO mice and their WT controls intermittently with PTH (1-34) or vehicle (saline) and their bone phenotype was evaluated in detail. In addition to bone histomorphometry, µ-CT analysis was kindly conducted by Mithila Vaidya of the laboratory of Prof. Reinhold Erben, Vienna, Austria. Furthermore, to investigate the role of AREG in bone development and homeostasis *in vivo*, the bone phenotype of 3- and 8-month-old AREG-KO and WT mice was analyzed by µ-CT. The results of the study were published in *Molecular and Cellular Endocrinology* (Jay *et al.*, 2015). In summary, our data indicate that AREG plays only a minor role in bone homeostasis in non-growing mice and is not required for the bone anabolic actions of intermittent PTH.

In AREG-KO mice, the deletion of exons 3 and 4 eliminates all three disulfide bounds, the heparin-binding region and the transmembrane domain of Pro-AREG. Additionally, splicing of exon 2 to exon 5 leads to a frameshift (Luetteke *et al.*, 1999). It was reported previously that AREG-KO mice show no alterations in growth or body weight, but female 4-week-old AREG-KO mice have less trabecular bone as compared to their WT control littermates (Luetteke *et al.*, 1999, Qin *et al.*, 2005). It has been described by Qin and co-workers that female 4-week-old AREG-KO mice have a reduced trabecular number, trabecular thickness, connectivity density and percent bone volume in the proximal tibia, and as a consequence an increased trabecular separation, whereas no differences were found in the cortical bone compartment (Qin *et al.*, 2005). In our study, µ-CT analysis showed that 3-month-old female AREG-KO mice had a mildly reduced cortical BMD and 8-month-old female AREG-KO mice showed a minor cortical thinning at the femoral midshaft as compared to WT controls. However, there were no differences in the trabecular bone compartment in the distal femoral metaphysis (Jay *et al.*, 2015). The different results between our study and that of Qin and co-workers are probably due to the different age of the animals (early puberty versus sexual maturity). Our data indicate that the lack of AREG does not lead to major abnormalities on cortical and trabecular bone on non-growing, sexually mature female mice (Jay *et al.*, 2015).

To investigate to which extent the lack of AREG might be functionally compensated by other EGFR ligands in bone cells *in vivo*, the expression levels in osteoblasts harvested

from the distal femoral metaphysis of male and female 3-week-old AREG-KO, heterozygous AREG$^{+/-}$ and WT mice were analyzed by qRT-PCR in our study. The expression levels of *Btc* and *Epgn* were decreased in osteoblasts of AREG-KO mice as compared to their controls. The mRNA expression level of *Ereg* remained unchanged, whereas the levels of *Egf* and *Hbegf* were significantly increased in osteoblasts of AREG-KO mice as compared to their controls. A similar tendency was seen in the mRNA levels of *Tgfa* (P=0.062) (Jay *et al.*, 2015). The increased expression levels of *Egf*, *Hbegf* and *Tgfa* in AREG-KO mice might, at least in part, be counterbalancing the effects of AREG deficiency and therefore explaining the only minor skeletal alterations in AREG-KO mice.

In line with these findings, it was previously reported that reduced expression of one EGFR-ligand can alter the expression levels of the other EGFR-ligands. In EPGN deficient mice, the expression of *Btc* was increased in testes and *Egf* expression was increased in kindney, lung and testes (Dahlhoff *et al.*, 2013). After hepatic injury, which leads to increased expression of *Areg*, the expression of *Tgfa*, *Egf* and *Btc* were decreased as compared to baseline levels, whereas the expression of *Ereg* was increased (Berasain and Avila, 2014, Berasain *et al.*, 2005).

In our study no differences in the femurs of male AREG-KO mice were found in pQCT analyses (unpublished data), indicating that the mild effects of AREG deficiency on cortical bone are sex-specific. In line with these findings, the reduction in trabecular bone volume in 4-week-old (pubescent) AREG-KO mice was only described in females (Qin *et al.*, 2005).

Skeletal sex-dependent differences in mice occur during puberty (3 to 8 weeks of age) and are characterized by a larger and stronger skeleton in male animals as compared to females (Callewaert *et al.*, 2010c). The sexual hormones estrogen and testosterone and their receptors are involved in the development of skeletal sexual dimorphism and have an important impact on skeletal growth and bone homeostasis (Callewaert *et al.*, 2010b). The primary female sex hormone estrogen limits periosteal bone expansion but stimulates endosteal bone apposition in females (Callewaert *et al.*, 2010b, Callewaert *et al.*, 2010c). Estrogen can act directly on bone cells and functional estrogen receptors are expressed in osteoblasts, osteocytes and osteoclasts (Riggs *et al.*, 2002, Braidman *et al.*, 2000, Eriksen *et al.*, 1988, Oursler *et al.*, 1991, Tomkinson *et*

al., 1998). *In vitro* studies showed that estrogen can increase proliferation and differentiation of mouse bone marrow derived osteoblastic-like cells, and it can increase osteoclast apoptosis (Qu *et al.*, 1998, Hughes *et al.*, 1996). Estrogen deficiency leads to an increased bone resorption and is a main reason for postmenopausal osteoporosis in elderly women (Riggs *et al.*, 2002, Manolagas, 2000). In addition to the actions of sex steroid hormones on bone, it is well established that growth hormone (GH, somatotropin) and IGF1 play a critical role in pubertal bone growth and in the development of skeletal sexual dimorphism. Estrogen can interact with IGF1 by increasing the expression of *Gh* and can therefore, in addition to its direct action on bone cells, indirectly modulate skeletal growth (Callewaert *et al.*, 2010b, Callewaert *et al.*, 2010c, Mauras *et al.*, 1996). In addition to the effects of sex on bone, it has been established that bone tissue has in its turn an influence on murine (and human) fertility, as the osteoblast specific hormone osteocalcin can modulate testosterone synthesis (Karsenty and Oury, 2014). Furthermore, estrogen can increase the expression of *Areg* and *Erbb2* in MCF-7 human breast carcinoma cells, indicating that *Areg* is an estrogen target gene *in vitro* (Vendrell *et al.*, 2004). Most recently, *Areg* has been identified as a key target gene of estrogen receptor positive breast cancer cells (Peterson *et al.*, 2015).

As in mice, the human male skeleton is larger and stronger than the female skeleton. Moreover, men do not experience menopause and therefore lose less bone during aging (Callewaert *et al.*, 2010a).

During menopause, the dropping levels of ovarian estrogen lead to accelerated bone loss and can cause postmenopausal osteoporosis (Cauley, 2014). Estrogen deficiency leads to an increased secretion of several bone-resorbing cytokines, such as IL1, IL6, tumor necrosis factor α (TNF), macrophage colony-stimulating factor (MCSF), and granulocyte-macrophage colony-stimulating factor (GMCSF) (Pacifici, 1996, Tella and Gallagher, 2014, Khosla *et al.*, 2012). Loss of estrogen also leads to an increased NF-κB activity in osteoblasts, resulting in a suppressed osteoblast activity and inhibited bone formation (Chang *et al.*, 2009, Khosla *et al.*, 2012).

There are two major approaches to treat osteoporosis: to prevent bone loss using anti resorptive agents (e.g. bisphosphonates, denosumab) and to stimulate bone formation with bone anabolic agents (e.g. strontium ranelate, teriparatide) (Tella and Gallagher,

2014). Bisphosphonates decrease bone turnover by inhibiting osteoclast formation. Denosumab is a monoclonal antibody, which specifically binds RANKL, hence suppressing osteoclast formation by inhibiting the binding of RANKL to its receptor RANK (Tella and Gallagher, 2014). Strontium renalate is, besides teriparatide, one of the few bone anabolic agents used in osteoporosis treatment. It stimulates bone formation by increasing osteoblast proliferation, but treatment with strontium renalate is contraindicated in patients with cardiovascular diseases (Canalis *et al.*, 1996, Marie *et al.*, 2001, Reginster *et al.*, 2015). Teriparatide contains recombinant human PTH (1-34) and can increase bone formation when injected intermittently (Poole and Reeve, 2005). Daily treatment with teriparatide rapidly increases bone mass and even weekly injections can lead to a bone anabolic effect (Sugiyama *et al.*, 2015).

However, the detailed mechanisms behind the bone anabolic actions of intermittent PTH treatment have not yet been fully understood. Several signaling pathways have been identified to play a role in mediating the bone anabolic effect of intermittent PTH treatment (Schneider *et al.*, 2012), e.g. IGF1 (Miyakoshi *et al.*, 2001), c-fos (Demiralp *et al.*, 2002), IL18 (Raggatt *et al.*, 2008), ß-arrestin 2 (Bouxsein *et al.*, 2005), sclerostin (Kramer *et al.*, 2010a) and the osteoclast regulating factor MCP1 (Tamasi *et al.*, 2013).

The bone anabolic effect of intermittent PTH was blunted in 5-week-old IGF1 deficient mice (Miyakoshi *et al.*, 2001), in 4-day-old c-fos deficient mice (Demiralp *et al.*, 2002), in 7- to 8-week old IL18 deficient mice (Raggatt *et al.*, 2008), in 4- and 6- month-old MCP1 deficient mice (in females to a lesser extent than in males) (Tamasi *et al.*, 2013) and in 8-week-old sclerostin deficient male mice and in 6-month-old sclerostin overexpressing mice (Kramer *et al.*, 2010b). In 13-week-old female and in 12-week-old male ß-arrestin 2 deficient mice the bone anabolic effect of intermittent PTH was altered and varied according to the sex (Bouxsein *et al.*, 2005, Ferrari *et al.*, 2005).

The EGFR ligand *Areg* was identified as a PTH target gene *in vitro* and *in vivo* (Qin et al., 2005). In rat UMR 106-01 osteoblastic cells *Areg* expression was increased more than 2-fold 4h and 12h after treatment with rat PTH (1-34) (Qin *et al.*, 2003). In rat calvarial osteoblasts, administration of rat PTH (1-34) increased the expression of *Areg* with the highest induction (23-fold) on day 14 (mineralization phase) and the lowest (5-fold) at day 6 (proliferative phase). The strongest induction was at 1h after administra-

tion in all three phases of proliferation, differentiation and mineralization, while the basal *Areg* expression levels did not change (Qin *et al.*, 2005). In mouse MC3T3 cells *Areg* expression was also increased after PTH treatment (Qin *et al.*, 2005). *In vivo*, intermittent treatment of 4-week-old male Sprague-Dawley rats with human PTH (1-38) increased *Areg* expression in the distal femoral metaphysis 12-fold after 1h and 2-fold after 4h (Qin *et al.*, 2005). *Areg* expression was also stimulated by other osteotropic hormones, such as prostaglandin E_2 and 1,25 dihydroxyvitamin D_3, in rat primary osteoblastic cells. Treatment of rat primary osteoblastic cells with prostaglandin E_2 increased *Areg* expression with a peak (13-fold) after 1h. Administration of 1,25 dihydroxyvitamin D_3 to rat primary osteoblastic cells increased *Areg* expression with a peak (24-fold) after 12h, but was lower at 1h (3-fold) and 4h (2-fold) (Qin *et al.*, 2005). Previously, other *in vitro* studies showed that *Areg* is also a 1,25 dihydroxyvitamin D_3 target gene in cells derived from a human squamous cell carcinoma and in human breast cancer cell lines (Akutsu *et al.*, 2001).

Furthermore, *in vitro* studies showed that AREG stimulates proliferation and prevents differentiation and mineralization of rat calvarial osteoblasts (Qin *et al.*, 2005). Addition of AREG to the medium of rat calvarial preosteoblastic cells increased their proliferation even in low concentrations (5ng/ml). Inhibition of the EGFR blocked this proliferative effect of AREG, indicating that this effect is mediated via EGFR signaling. The presence of ß-glycerolphosphate and ascorbic acid usually induces differentiation and mineralization of calvarial osteoblasts, which start to build bone nodules (Qin *et al.*, 2005). Administration of AREG to the medium either from day 1 or day 7 to day 20 completely inhibited differentiation, as there was no formation of bone nodules. Analysis of RNA harvested from these day 20 cultures showed an increase in the expression of several bone markers, such as *Mmp13*, alkaline phosphatase, osteocalcin and osteonectin in AREG-treated cells as compared to untreated cells (Qin *et al.*, 2005). AREG also stimulated the phosphorylation of AKT and ERK, two major downstream signaling pathways activated by the EGFR, and increased the expression of *c-jun* and *c-fos*, whose expression can be activated by phosphorylated ERK (Qin *et al.*, 2005).

AREG was also identified as a chemotactic factor for mesenchymal progenitors (Zhu *et al.*, 2012). PTH treatment leads to release of AREG from osteoblastic cells, which promotes the migration of mesenchymal progenitors *in vitro* via AKT and p38MAPK pathways (Zhu *et al.*, 2012). In the same study it was shown that the bone anabolic

effect was blunted in EGFR$^{wa5/flox}$ Col 3.6-Cre mice, indicating that the bone anabolic properties of intermittent PTH require EGFR signaling. However, the bone anabolic effect was fully maintained in heterozygous Wa5 mice, most likely due to residual EGFR activity in these animals (Schneider *et al.*, 2012).

AREG seems to be the major EGFR ligand mediating the bone anabolic effect of PTH (Schneider *et al.*, 2009b). To investigate the role of AREG in mediating the bone anabolic actions of PTH, we treated 3-month-old female AREG-KO and WT mice intermittently with PTH or vehicle (physiological saline) five times a week over a period of four weeks and analyzed their bone phenotype in detail.

Surprisingly, the bone anabolic effect of PTH was fully maintained in female AREG-KO mice in our study (Jay *et al.*, 2015). In the femoral midshaft, microground histological sections revealed a strong increase in the cortical thickness in PTH-treated AREG-KO and WT mice as compared to their saline-treated controls. µ-CT analysis confirmed a higher BMD and cortical thickness in the femoral midshaft of the PTH-treated mice (Jay *et al.*, 2015). There were no differences in the PTH-mediated increase of cortical BMD and cortical thickness between AREG-KO and WT mice. In line with the previous findings in 3- and 8-month-old AREG-KO mice, there was a small reduction in the cortical BMD and cortical thickness in the vehicle-treated AREG-KO mice as compared to their WT controls (Jay *et al.*, 2015). PTH treatment profoundly increased the amount of newly formed periosteal and endocortical bone. Measurement of the periosteal and endocortical mineral apposition rate (MAR) showed a marked increase in the bone formation over the four weeks of experiment in both WT and AREG-KO mice.

In the distal femoral metaphysis intermittent PTH treatment led to an increase in BMD, trabecular thickness and bone formation rate (BFR) in both AREG-KO and WT mice as compared to their saline-treated controls (Jay *et al.*, 2015). Consistent with the previous results in 3- and 8-month-old mice, no differences were observed in the trabecular bone compartment between vehicle-treated AREG-KO and WT mice.

The number of osteoclasts per bone perimeter was lower in PTH-treated AREG-KO mice as compared to PTH-treated WT mice. It is known that intermittent PTH treatment leads to higher expression levels of *Rankl*, resulting in an increased osteoclast formation and therefore bone resorption, most likely to sustain the balance between bone formation and bone resorption (Li *et al.*, 2007a). Osteoclasts do not express functional

EGFR, but it was shown by Zhu and co-workers that EGFR ligands can indirectly increase osteoclast recruitment by modulating the expression of *Mcp1* and *Opg* (Zhu *et al.*, 2007). EGFR ligands can stimulate the expression of *Mcp1* in osteoblasts, resulting in an increased osteoclast formation (Zhu *et al.*, 2007). Additionally, it has to be mentioned that *Rankl*, whose expression is increased by intermittent PTH treatment, also stimulates *Mcp1* expression and can therefore not only directly, but also indirectly promote osteoclastogenesis (Kim *et al.*, 2005, Li *et al.*, 2007a). EGFR ligands seem to have no apparent effect on *Rankl* expression in osteoblastic cells (Kim *et al.*, 2005). Furthermore, EGFR ligands can inhibit the expression of *Opg* and further increase osteoclast formation (Zhu *et al.*, 2007). Normally, OPG acts as a decoy receptor for RANKL and blocks its binding to RANK, leading to a reduced osteoclast formation (Boyle *et al.*, 2003). Moreover, it has been reported that EGFR-KO mice have delayed osteoclast recruitment into the hypertrophic cartilage, and a reduced osteoclast number was observed at the border to the bone marrow space in TGFA-KO mice and in mice with a reduced EGFR activity specifically in chondrocytes (Usmani *et al.*, 2012, Wang *et al.*, 2004, Zhang *et al.*, 2013). In line with these findings, our data indicate that the absence of AREG leads to a reduced recruitment of osteoclasts and therefore to a reduced bone resorption under PTH-mediated bone anabolic conditions, while the BFR was similar to that of PTH-treated WT mice. However, this reduction in bone resorption did not translate into a stronger bone anabolic effect in PTH-treated AREG-KO mice in comparison to PTH-treated WT mice (Jay *et al.*, 2015).

To evaluate the effects of intermittent PTH treatment at the whole body level, we measured the serum levels of osteocalcin. Osteocalcin is a non-collagenous protein preferentially expressed by mature, mineralized osteoblasts, and used as a marker for bone formation, since it directly reflects the level of osteoblast formation and activity (Neve *et al.*, 2013, Chapurlat and Confavreux, 2016). In vitro studies showed that PTH can promote osteocalcin transcription in osteoblastic-like cells (Yu and Chandrasekhar, 1997). Osteocalcin is also released by osteoclasts *in vitro*, and administration of PTH increases the levels of osteocalcin in osteoclasts (Ivaska *et al.*, 2004). The levels of serum osteocalcin were similarly increased in the PTH-treated WT and AREG-KO mice as compared to their vehicle-treated controls. This finding further indicates that the lack of AREG does not impair the bone anabolic effect of intermittent PTH treatment, not only at the femur but possibly also on the whole body level (Jay *et al.*, 2015).

The level of urinary collagen crosslink deoxypyridinoline (DPD) was unchanged between the groups. Urinary DPD is a product of collagen degradation and is used as a marker for bone resorption (Vesper *et al.*, 2003). However, a possible effect of intermittent PTH treatment on bone resorption could not be assessed with this marker.

Previously it was shown by Zhang and co-workers that the bone anabolic action of intermittent PTH was blunted in in EGFR$^{wa5/flox}$ Col 3.6-Cre mice, indicating that this effect requires signaling via the EGFR (Zhu *et al.*, 2012). AREG was assumed to be the most important ligand of the EGFR in bone and was identified as a PTH target gene *in vitro* and *in vivo* (Qin *et al.*, 2003, Qin *et al.*, 2005). Surprisingly, the bone anabolic response was fully maintained in AREG-KO mice. It is likely that other pathways and growth factors might compensate the lack of AREG. Microarray analysis identified *Tgfa* as a PTH-regulated gene (Qin *et al.*, 2003). In UMR 106-01 osteoblastic cells *Tgfa* expression was increased 2.5-fold 4h after PTH treatment. The expression of the proto-oncogene *c-fos*, whose transcription can be activated via EGFR signaling, was also found to be upregulated in this study (7-fold after 4h, 2.5-fold after 12h) (Qin *et al.*, 2003, Schneider *et al.*, 2009b). It is possible that in absence of AREG, TGFA or other EGFR ligands can mediate the bone anabolic effect of PTH via the EGFR.

Several studies showed that EGFR signaling leads to an anabolic effect in bone. 3-month-old EGFR$^{wa5/flox}$ Col 3.6-Cre mice have shorter femurs and a significantly reduced total BMD, trabecular BMD and cortical thickness (Zhang *et al.*, 2011b). Vice versa, mice with a constitutively activation and increased signaling of the EGFR have a higher trabecular BMD in both sexes, and a higher total BMD in females (Fitch *et al.*, 2003, Zhang *et al.*, 2011b). However, 6-month-old female Dsk5 mice do not exhibit a bone phenotype, while there is still a profound increase in bone volume in age-matched male Dsk5 mice, indicating that sex-specific factors, e.g. estrogen, might influence the effects of EGFR signaling in bone (Zhang *et al.*, 2011b). In line with the findings in osteoblast-specific EGFR-KO mice, 3-month-old heterozygous Wa5 mice in a C57BL/6 background have a reduced total BMD in femurs and lumbar vertebral bodies (Schneider *et al.*, 2012). In a different genetic background (129S1/SvImJ) 1- and 3-month-old heterozygous Wa5 mice did not develop a bone phenotype (Zhang *et al.*, 2011b). Such phenotypic variations depending on the genetic background have been

reported earlier in total EGFR-KO mice (Sibilia and Wagner, 1995, Threadgill *et al.*, 1995).

While lack of AREG leads to a reduced trabecular bone mass in 4-week-old female mice and to slightly reduced BMD and minor cortical thinning in sexually mature female mice, *Areg* overexpression leads to a transient increase in the trabecular bone mass (Qin *et al.*, 2005, Vaidya *et al.*, 2015, Jay *et al.*, 2015). Mice with an osteoblast-specific overexpression of *Areg* under the control of the 2.3kb collagen α1 promoter (COL1-AREG) showed an increased trabecular BMD in the distal femoral metaphysis at 4, 8, and 10 weeks of age as compared to WT controls (Vaidya *et al.*, 2015). However, the bone phenotype was transient and completely disappeared in 5- and 18-month-old mice. No differences were found in the femoral midshaft and in the lumbar vertebrae between COL1-AREG and WT mice, indicating that the effects of *Areg* overexpression are site-specific and growth-related. The number of osteoclasts was significantly lower in 4-week-old COL1-AREG mice, while the trabecular BFR remained unchanged, indicating that the transient increase in trabecular BMD is due to a reduced bone resorption (Vaidya *et al.*, 2015). These data demonstrate that EGFR ligands can not only stimulate osteoclastogenesis, but that an increased EGFR activity in consequence of AREG overabundance can also decrease osteoclast formation (Zhu *et al.*, 2007, Vaidya *et al.*, 2015). Furthermore, *in vitro* studies with mouse calvarial osteoblasts showed that *Areg* overexpression did not change osteoblast differentiation or proliferation (Vaidya *et al.*, 2015).

In conclusion, our data suggest that AREG is dispensable for the bone anabolic actions of intermittent PTH treatment. AREG plays only a minor role in bone development, and lack of AREG results in a reduced cortical thickness and cortical BMD in sexually mature female mice (Jay *et al.*, 2015).

Analysis of the expression levels of the other EGFR ligands in AREG-KO osteoblasts revealed an increased expression of *Egf* and *Hbegf* and a similar trend was seen for *Tgfa*. The latter is of particular interest, because *Tgfa* was previously reported to be a PTH target gene in osteoblasts. Microarray analysis showed that *Tgfa* expression was increased in rat UMR 106-01 osteoblastic cells after PTH treatment (Qin *et al.*, 2003). Both *Hbegf* and *Tgfa* have been previously reported to be PTH-regulated target genes

in rat UMR 106-01 osteoblastic cells (Qin *et al.*, 2005). Future analysis of the expression levels of the other EGFR ligands in AREG deficient osteoblasts under PTH-mediated bone anabolic conditions will help to gain a greater knowledge about the ability of the other ligands to compensate the lack of AREG. *In vivo* studies, assessing the role of TGFA alone and in combination with AREG, will help to gain greater insight in the role of EGFR signaling in mediating the bone anabolic actions of intermittent PTH treatment.

To further understand the underlying mechanisms of the bone anabolic effect of PTH, future work needs to assess the role of EGFR signaling in bone in combination with the closely related ERBB2 receptor, which is the preferred heterodimerization partner of EGFR and the EGFR family member with the highest expression in bone cells (Citri and Yarden, 2006, Genetos *et al.*, 2010, Jay *et al.*, 2015).

6 Summary

Parathyroid hormone (PTH) is a key regulator of bone remodeling and calcium homeostasis. It is well established that PTH, in contrast to its classical bone catabolic actions, can also act as a bone anabolic agent when administered intermittently (Tam *et al.*, 1982, Poole and Reeve, 2005).

In recent years, numerous signaling pathways and molecules have been proposed as mediators of this paradoxical action. However, the detailed mechanisms remain largely unknown. Amphiregulin (AREG), a ligand of the epidermal growth factor receptor (EGFR) has been identified as a PTH target gene *in vitro* and *in vivo*, and there is accumulating evidence that the bone anabolic actions of PTH might be, at least in part, mediated via AREG-EGFR-signaling (Schneider *et al.*, 2009b, Qin *et al.*, 2005). *Areg* expression was highly increased in UMR 106-01 osteoblastic cells, primary rat calvarial osteoblasts, mouse MC3T3 cells and in the femoral metaphysis of young male rats after PTH treatment (Qin *et al.*, 2003, Qin *et al.*, 2005). Furthermore, AREG stimulates proliferation and inhibits differentiation and mineralization of osteoblasts and *Areg* expression is also increased by other osteotropic hormones, such as prostaglandin E_2 and 1,25-dihydroxyvitamin D_3 (Qin *et al.*, 2005). Mice lacking AREG show no alterations in growth but they have been reported to have less trabecular bone as compared to controls (Qin *et al.*, 2005, Luetteke *et al.*, 1999). Vice versa, mice overexpressing *Areg* specifically in osteoblasts showed a transient increase of bone mass in the trabecular bone compartment (Vaidya *et al.*, 2015). Taken together, these data indicate that AREG seems to be the major EGFR-ligand in mediating the bone anabolic properties of intermittent PTH.

To clarify to which extent AREG is required for the bone anabolic actions of PTH *in vivo*, we treated 3-month-old female global AREG knockout (AREG-KO) mice and controls with 80µg/kg PTH (1-34) or vehicle (physiological saline) five times per week over four weeks and analyzed their bone phenotype via bone histomorphometry. Additionally, we analyzed the levels of serum osteocalcin, a marker for bone formation, and urinary deoxypyridinoline, a marker for bone resorption.

Intermittent PTH treatment of AREG-KO mice led to an increased bone formation of trabecular and cortical bone, which was comparable to the effect in control animals. Hence, the bone anabolic effect was fully maintained in AREG-KO mice. Surprisingly, the number of osteoclasts per bone perimeter was decreased in PTH-treated AREG-KO mice relative to their respective wildtype controls, indicating that lack of AREG leads to a reduced osteoclastogenesis under PTH-mediated bone anabolic conditions. However, this reduction did not translate into a stronger bone anabolic effect in AREG-KO mice. The levels of serum osteocalcin were increased in both PTH-treated groups as compared to their vehicle-treated controls, suggesting that PTH might lead to an increased bone anabolism at the whole body level in both wildtype and AREG-KO mice. The urinary levels of deoxypyridinoline remained unchanged between the groups, indicating that the effect of PTH on bone resorption could not be assessed with this marker.

In conclusion, our data indicate that AREG is dispensable for the bone anabolic effect of intermittent PTH, at least in 3-month-old female mice.

7 Zusammenfassung

Parathormon (PTH) ist ein Hauptregulator des Knochenstoffwechsels und der Calciumhomöostase. Es ist allgemein bekannt, dass PTH im Gegensatz zu seiner klassischen knochenkatabolen Eigenschaft auch knochenanabol wirken kann, wenn es intermittierend verabreicht wird (Tam *et al.*, 1982, Poole and Reeve, 2005).

In den letzten Jahren wurden von zahlreichen Signalwegen und Moleküle vermutet, dass sie diesen paradoxen Effekt vermitteln. Die genauen Mechanismen sind jedoch immer noch weitestgehend unbekannt. Amphiregulin (AREG), ein Ligand des Epidermal Growth Factor Receptors (EGFR), wurde *in vitro* und *in vivo* als PTH-reguliertes Gen identifiziert, und es gibt zunehmend Hinweise darauf, dass die knochenanabole Wirkung von PTH zumindest teilweise über den AREG-EGFR-Signalweg vermittelt sein könnte (Schneider *et al.*, 2009b, Qin *et al.*, 2005). Die Expression von *Areg* war in UMR 106-01 osteoblasten-ähnlichen Zellen, in primären Osteoblasten aus Ratten-Calvarien, in Maus-MC3T3 Zellen und in der Metaphyse des Femurs junger männlicher Ratten nach PTH-Behandlung stark erhöht (Qin *et al.*, 2003, Qin *et al.*, 2005). Zudem stimuliert AREG die Proliferation von Osteoblasten, während es ihre Differenzierung und Mineralisation hemmt. Auch andere osteotrope Hormone, wie Prostaglandin E_2 und 1,25-Dihydroxyvitamin D_3, erhöhen die Expression von *Areg* (Qin *et al.*, 2005). Mäuse, denen AREG fehlt, zeigen kein verändertes Wachstum, aber sie haben weniger trabekulären Knochen im Vergleich zu Kontrolltieren (Qin *et al.*, 2005, Luetteke *et al.*, 1999). Umgekehrt zeigen Mäuse mit osteoblasten-spezifischer Überexpression von *Areg* einen transienten Anstieg der trabekulären Knochenmasse (Vaidya *et al.*, 2015). All diese Daten weisen darauf hin, dass AREG vermutlich der wichtigste Ligand des EGFR ist, der die knochenanabolen Eigenschaften von intermittierend verabreichtem PTH vermittelt.

Um zu klären, inwieweit AREG für die knochenanabole Wirkung von PTH *in vivo* benötigt wird, wurden 3 Monate alte weibliche ubiquitäre AREG-Knockout Mäuse (AREG-KO) und Kontrolltiere mit 80µg/kg PTH (1-34) oder Trägersubstanz (physiologische Kochsalzlösung) fünfmal die Woche für vier Wochen behandelt, und der Knochenphä-

notyp histomorphometrisch ausgewertet. Zusätzlich wurde die Osteocalcin-Konzentration im Serum, ein Marker für die Knochenformation, und die Deoxypyridinoline-Konzentration im Urin, ein Marker für die Knochenresorption, gemessen.

Die intermittierende Behandlung mit PTH führte zu einer erhöhten kortikalen und trabekulären Knochenneubildung in AREG-KO Mäusen, die mit der in Kontrollmäusen vergleichbar war. Der knochenanabole Effekt war also in AREG-KO Mäusen in vollem Umfang erhalten. Überraschenderweise war die Anzahl der Osteoklasten in Relation zum Knochenumfang in den mit PTH behandelten AREG-KO Mäusen niedriger als in der entsprechenden Wildtyp-Kontrollgruppe. Dies lässt darauf schließen, dass in Abwesenheit von AREG unter PTH-vermittelten knochenanabolen Bedingungen weniger Osteoklasten gebildet werden. Diese Reduktion führte jedoch nicht zu einem stärkeren knochenanabolen Effekt in AREG-KO Mäusen. In beiden mit PTH behandelten Gruppen war im Vergleich zu den mit Trägersubstanz behandelten Kontrollgruppen ein Anstieg an Osteocalcin im Serum feststellbar. Dies weist darauf hin, dass PTH sowohl bei AREG-KO Mäusen als auch bei Kontrolltieren im gesamten Körper knochenanabol wirken könnte. Die im Urin gemessenen Werte von Deoxypyridinoline unterschieden sich nicht zwischen den Gruppen, was vermuten lässt, dass der Einfluss der PTH-Behandlung auf die Knochenresorption mit diesem Marker nicht erfasst werden konnte.

Zusammengefasst deuten unsere Daten darauf hin, dass AREG für den knochenanabolen Effekt, zumindest in 3 Monate alten weiblichen Mäusen, nicht benötigt wird.

8 References

AKUTSU, N., BASTIEN, Y., LIN, R., MADER, S. & WHITE, J. H. 2001. Amphiregulin is a vitamin D3 target gene in squamous cell and breast carcinoma. *Biochem Biophys Res Commun,* 281**,** 1051-6.

ANGELUCCI, A., GRAVINA, G. L., RUCCI, N., MILLIMAGGI, D., FESTUCCIA, C., MUZI, P., TETI, A., VICENTINI, C. & BOLOGNA, M. 2006. Suppression of EGF-R signaling reduces the incidence of prostate cancer metastasis in nude mice. *Endocr Relat Cancer,* 13**,** 197-210.

ARTEAGA, C. L. & ENGELMAN, J. A. 2014. ERBB receptors: from oncogene discovery to basic science to mechanism-based cancer therapeutics. *Cancer Cell,* 25**,** 282-303.

BELLIDO, T., ALI, A. A., PLOTKIN, L. I., FU, Q., GUBRIJ, I., ROBERSON, P. K., WEINSTEIN, R. S., O'BRIEN, C. A., MANOLAGAS, S. C. & JILKA, R. L. 2003. Proteasomal degradation of Runx2 shortens parathyroid hormone-induced anti-apoptotic signaling in osteoblasts. A putative explanation for why intermittent administration is needed for bone anabolism. *J Biol Chem,* 278**,** 50259-72.

BERASAIN, C. & AVILA, M. A. 2014. Amphiregulin. *Semin Cell Dev Biol*.

BERASAIN, C., CASTILLO, J., PERUGORRIA, M. J., PRIETO, J. & AVILA, M. A. 2007. Amphiregulin: a new growth factor in hepatocarcinogenesis. *Cancer Lett,* 254**,** 30-41.

BERASAIN, C., GARCIA-TREVIJANO, E. R., CASTILLO, J., ERROBA, E., SANTAMARIA, M., LEE, D. C., PRIETO, J. & AVILA, M. A. 2005. Novel role for amphiregulin in protection from liver injury. *J Biol Chem,* 280**,** 19012-20.

BOUXSEIN, M. L., PIERROZ, D. D., GLATT, V., GODDARD, D. S., CAVAT, F., RIZZOLI, R. & FERRARI, S. L. 2005. beta-Arrestin2 regulates the differential response of cortical and trabecular bone to intermittent PTH in female mice. *J Bone Miner Res,* 20**,** 635-43.

BOYLE, W. J., SIMONET, W. S. & LACEY, D. L. 2003. Osteoclast differentiation and activation. *Nature,* 423**,** 337-42.

BRAIDMAN, I., BARIS, C., WOOD, L., SELBY, P., ADAMS, J., FREEMONT, A. & HOYLAND, J. 2000. Preliminary evidence for impaired estrogen receptor-alpha protein expression in osteoblasts and osteocytes from men with idiopathic osteoporosis. *Bone,* 26**,** 423-7.

BUSSER, B., SANCEY, L., BRAMBILLA, E., COLL, J. L. & HURBIN, A. 2011. The multiple roles of amphiregulin in human cancer. *Biochim Biophys Acta,* 1816**,** 119-31.

CALLEWAERT, F., BOONEN, S. & VANDERSCHUEREN, D. 2010a. Sex steroids and the male skeleton: a tale of two hormones. *Trends Endocrinol Metab,* 21**,** 89-95.

CALLEWAERT, F., SINNESAEL, M., GIELEN, E., BOONEN, S. & VANDERSCHUEREN, D. 2010b. Skeletal sexual dimorphism: relative contribution of sex steroids, GH-IGF1, and mechanical loading. *J Endocrinol,* 207**,** 127-34.

CALLEWAERT, F., VENKEN, K., KOPCHICK, J. J., TORCASIO, A., VAN LENTHE, G. H., BOONEN, S. & VANDERSCHUEREN, D. 2010c. Sexual dimorphism in cortical bone size and strength but not density is determined by independent and time-specific actions of sex steroids and IGF-1: evidence from pubertal mouse models. *J Bone Miner Res,* 25**,** 617-26.

CANALIS, E., HOTT, M., DELOFFRE, P., TSOUDEROS, Y. & MARIE, P. J. 1996. The divalent strontium salt S12911 enhances bone cell replication and bone formation in vitro. *Bone,* 18**,** 517-23.

CAULEY, J. A. 2014. Estrogen and bone health in men and women. *Steroids*.

CHAN, S. Y. & WONG, R. W. 2000. Expression of epidermal growth factor in transgenic mice causes growth retardation. *J Biol Chem,* 275**,** 38693-8.

CHANDRA, A., LAN, S., ZHU, J., SICLARI, V. A. & QIN, L. 2013. Epidermal growth factor receptor (EGFR) signaling promotes proliferation and survival in osteoprogenitors by increasing early growth response 2 (EGR2) expression. *J Biol Chem,* 288**,** 20488-98.

CHANG, J., WANG, Z., TANG, E., FAN, Z., MCCAULEY, L., FRANCESCHI, R., GUAN, K., KREBSBACH, P. H. & WANG, C. Y. 2009. Inhibition of osteoblastic bone formation by nuclear factor-kappaB. *Nat Med,* 15**,** 682-9.

CHAPURLAT, R. D. & CONFAVREUX, C. B. 2016. Novel biological markers of bone: from bone metabolism to bone physiology. *Rheumatology (Oxford)*.

CITRI, A. & YARDEN, Y. 2006. EGF-ERBB signalling: towards the systems level. *Nat Rev Mol Cell Biol,* 7**,** 505-16.

CLARKE, B. 2008. Normal bone anatomy and physiology. *Clin J Am Soc Nephrol,* 3 Suppl 3**,** S131-9.

COOK, P. W., PIEPKORN, M., CLEGG, C. H., PLOWMAN, G. D., DEMAY, J. M., BROWN, J. R. & PITTELKOW, M. R. 1997. Transgenic expression of the human amphiregulin gene induces a psoriasis-like phenotype. *J Clin Invest,* 100**,** 2286-94.

DAHLHOFF, M., SCHAFER, M., WOLF, E. & SCHNEIDER, M. R. 2013. Genetic deletion of the EGFR ligand epigen does not affect mouse embryonic development and tissue homeostasis. *Exp Cell Res,* 319**,** 529-35.

DAHLHOFF, M., WOLF, E. & SCHNEIDER, M. R. 2014. The ABC of BTC: structural properties and biological roles of betacellulin. *Semin Cell Dev Biol,* 28**,** 42-8.

DEMIRALP, B., CHEN, H. L., KOH, A. J., KELLER, E. T. & MCCAULEY, L. K. 2002. Anabolic actions of parathyroid hormone during bone growth are dependent on c-fos. *Endocrinology,* 143**,** 4038-47.

DI LORENZO, G., TORTORA, G., D'ARMIENTO, F. P., DE ROSA, G., STAIBANO, S., AUTORINO, R., D'ARMIENTO, M., DE LAURENTIIS, M., DE PLACIDO, S., CATALANO, G., BIANCO, A. R. & CIARDIELLO, F. 2002. Expression of epidermal growth factor receptor correlates with disease relapse and progression to androgen-independence in human prostate cancer. *Clin Cancer Res,* 8**,** 3438-44.

DOBASHI, Y., SUZUKI, S., SUGAWARA, H. & OOI, A. 2007. Involvement of epidermal growth factor receptor and downstream molecules in bone and soft tissue tumors. *Hum Pathol,* 38**,** 914-25.

DOBNIG, H. & TURNER, R. T. 1995. Evidence that intermittent treatment with parathyroid hormone increases bone formation in adult rats by activation of bone lining cells. *Endocrinology,* 136**,** 3632-8.

ERBEN, R. G. 1997. Embedding of bone samples in methylmethacrylate: an improved method suitable for bone histomorphometry, histochemistry, and immunohistochemistry. *J Histochem Cytochem,* 45**,** 307-13.

ERIKSEN, E. F., COLVARD, D. S., BERG, N. J., GRAHAM, M. L., MANN, K. G., SPELSBERG, T. C. & RIGGS, B. L. 1988. Evidence of estrogen receptors in normal human osteoblast-like cells. *Science,* 241**,** 84-6.

FERRARI, S. L., PIERROZ, D. D., GLATT, V., GODDARD, D. S., BIANCHI, E. N., LIN, F. T., MANEN, D. & BOUXSEIN, M. L. 2005. Bone response to intermittent parathyroid hormone is altered in mice null for {beta}-Arrestin2. *Endocrinology,* 146**,** 1854-62.

FITCH, K. R., MCGOWAN, K. A., VAN RAAMSDONK, C. D., FUCHS, H., LEE, D., PUECH, A., HERAULT, Y., THREADGILL, D. W., HRABE DE ANGELIS, M. & BARSH, G. S. 2003. Genetics of dark skin in mice. *Genes Dev,* 17**,** 214-28.

FURUGAKI, K., MORIYA, Y., IWAI, T., YOROZU, K., YANAGISAWA, M., KONDOH, K., FUJIMOTO-OHUCHI, K. & MORI, K. 2011. Erlotinib inhibits osteolytic bone invasion of human non-small-cell lung cancer cell line NCI-H292. *Clin Exp Metastasis,* 28**,** 649-59.

GENETOS, D. C., RAO, R. R. & VIDAL, M. A. 2010. Betacellulin inhibits osteogenic differentiation and stimulates proliferation through HIF-1alpha. *Cell Tissue Res,* 340**,** 81-9.

GILMORE, J. L., SCOTT, J. A., BOUIZAR, Z., ROBLING, A., PITFIELD, S. E., RIESE, D. J., 2ND & FOLEY, J. 2008. Amphiregulin-EGFR signaling regulates PTHrP gene expression in breast cancer cells. *Breast Cancer Res Treat,* 110**,** 493-505.

HARRIS, R. C., CHUNG, E. & COFFEY, R. J. 2003. EGF receptor ligands. *Exp Cell Res,* 284**,** 2-13.

HIGGINBOTHAM, J. N., DEMORY BECKLER, M., GEPHART, J. D., FRANKLIN, J. L., BOGATCHEVA, G., KREMERS, G. J., PISTON, D. W., AYERS, G. D., MCCONNELL, R. E., TYSKA, M. J. & COFFEY, R. J. 2011. Amphiregulin exosomes increase cancer cell invasion. *Curr Biol,* 21**,** 779-86.

HINKLE, C. L., SUNNARBORG, S. W., LOISELLE, D., PARKER, C. E., STEVENSON, M., RUSSELL, W. E. & LEE, D. C. 2004. Selective roles for tumor necrosis factor alpha-converting enzyme/ADAM17 in the shedding of the epidermal growth factor receptor ligand family: the juxtamembrane stalk determines cleavage efficiency. *J Biol Chem,* 279**,** 24179-88.

HOCK, J. M., GERA, I., FONSECA, J. & RAISZ, L. G. 1988. Human parathyroid hormone-(1-34) increases bone mass in ovariectomized and orchidectomized rats. *Endocrinology,* 122**,** 2899-904.

HUGHES, D. E., DAI, A., TIFFEE, J. C., LI, H. H., MUNDY, G. R. & BOYCE, B. F. 1996. Estrogen promotes apoptosis of murine osteoclasts mediated by TGF-beta. *Nat Med,* 2**,** 1132-6.

ISOKANE, M., HIEDA, M., HIRAKAWA, S., SHUDOU, M., NAKASHIRO, K., HASHIMOTO, K., HAMAKAWA, H. & HIGASHIYAMA, S. 2008. Plasma-membrane-anchored growth factor pro-amphiregulin binds A-type lamin and regulates global transcription. *J Cell Sci,* 121**,** 3608-18.

IVASKA, K. K., HENTUNEN, T. A., VAARANIEMI, J., YLIPAHKALA, H., PETTERSSON, K. & VAANANEN, H. K. 2004. Release of intact and fragmented osteocalcin molecules from bone matrix during bone resorption in vitro. *J Biol Chem,* 279**,** 18361-9.

JAY, F. F., VAIDYA, M., PORADA, S. M., ANDRUKHOVA, O., SCHNEIDER, M. R. & ERBEN, R. G. 2015. Amphiregulin lacks an essential role for the bone anabolic action of parathyroid hormone. *Mol Cell Endocrinol*.

JILKA, R. L., WEINSTEIN, R. S., BELLIDO, T., ROBERSON, P., PARFITT, A. M. & MANOLAGAS, S. C. 1999. Increased bone formation by prevention of osteoblast apoptosis with parathyroid hormone. *J Clin Invest,* 104**,** 439-46.

KARSENTY, G. & OURY, F. 2014. Regulation of male fertility by the bone-derived hormone osteocalcin. *Mol Cell Endocrinol,* 382**,** 521-6.

KARSENTY, G. & WAGNER, E. F. 2002. Reaching a genetic and molecular understanding of skeletal development. *Dev Cell,* 2**,** 389-406.

KHOSLA, S., OURSLER, M. J. & MONROE, D. G. 2012. Estrogen and the skeleton. *Trends Endocrinol Metab,* 23**,** 576-81.

KIM, M. S., DAY, C. J. & MORRISON, N. A. 2005. MCP-1 is induced by receptor activator of nuclear factor-{kappa}B ligand, promotes human osteoclast fusion, and rescues granulocyte macrophage colony-stimulating factor suppression of osteoclast formation. *J Biol Chem,* 280**,** 16163-9.

KRAMER, I., KELLER, H., LEUPIN, O. & KNEISSEL, M. 2010a. Does osteocytic SOST suppression mediate PTH bone anabolism? *Trends Endocrinol Metab,* 21**,** 237-44.

KRAMER, I., LOOTS, G. G., STUDER, A., KELLER, H. & KNEISSEL, M. 2010b. Parathyroid hormone (PTH)-induced bone gain is blunted in SOST overexpressing and deficient mice. *J Bone Miner Res,* 25**,** 178-89.

LEE, D., CROSS, S. H., STRUNK, K. E., MORGAN, J. E., BAILEY, C. L., JACKSON, I. J. & THREADGILL, D. W. 2004. Wa5 is a novel ENU-induced antimorphic allele of the epidermal growth factor receptor. *Mamm Genome,* 15**,** 525-36.

LI, X., LIU, H., QIN, L., TAMASI, J., BERGENSTOCK, M., SHAPSES, S., FEYEN, J. H., NOTTERMAN, D. A. & PARTRIDGE, N. C. 2007a. Determination of dual effects of parathyroid hormone on skeletal gene expression in vivo by microarray and network analysis. *J Biol Chem,* 282**,** 33086-97.

LI, X., QIN, L., BERGENSTOCK, M., BEVELOCK, L. M., NOVACK, D. V. & PARTRIDGE, N. C. 2007b. Parathyroid hormone stimulates osteoblastic expression of MCP-1 to recruit and increase the fusion of pre/osteoclasts. *J Biol Chem,* 282**,** 33098-106.

LIU, J. F., TSAO, Y. T. & HOU, C. H. 2015. Amphiregulin enhances intercellular adhesion molecule-1 expression and promotes tumor metastasis in human osteosarcoma. *Oncotarget*.

LONG, F. 2012. Building strong bones: molecular regulation of the osteoblast lineage. *Nat Rev Mol Cell Biol,* 13**,** 27-38.

LUETTEKE, N. C., QIU, T. H., FENTON, S. E., TROYER, K. L., RIEDEL, R. F., CHANG, A. & LEE, D. C. 1999. Targeted inactivation of the EGF and amphiregulin genes reveals distinct roles for EGF receptor ligands in mouse mammary gland development. *Development,* 126**,** 2739-50.

MANOLAGAS, S. C. 2000. Birth and death of bone cells: basic regulatory mechanisms and implications for the pathogenesis and treatment of osteoporosis. *Endocr Rev,* 21**,** 115-37.

MARIE, P. J., AMMANN, P., BOIVIN, G. & REY, C. 2001. Mechanisms of action and therapeutic potential of strontium in bone. *Calcif Tissue Int,* 69**,** 121-9.

MAURAS, N., ROGOL, A. D., HAYMOND, M. W. & VELDHUIS, J. D. 1996. Sex steroids, growth hormone, insulin-like growth factor-1: neuroendocrine and metabolic regulation in puberty. *Horm Res,* 45**,** 74-80.

MIETTINEN, P. J., BERGER, J. E., MENESES, J., PHUNG, Y., PEDERSEN, R. A., WERB, Z. & DERYNCK, R. 1995. Epithelial immaturity and multiorgan failure in mice lacking epidermal growth factor receptor. *Nature,* 376**,** 337-41.

MIETTINEN, P. J., CHIN, J. R., SHUM, L., SLAVKIN, H. C., SHULER, C. F., DERYNCK, R. & WERB, Z. 1999. Epidermal growth factor receptor function is necessary for normal craniofacial development and palate closure. *Nat Genet,* 22**,** 69-73.

MISHRA, A., SHIOZAWA, Y., PIENTA, K. J. & TAICHMAN, R. S. 2011. Homing of cancer cells to the bone. *Cancer Microenviron,* 4**,** 221-35.

MIYAKOSHI, N., KASUKAWA, Y., LINKHART, T. A., BAYLINK, D. J. & MOHAN, S. 2001. Evidence that anabolic effects of PTH on bone require IGF-I in growing mice. *Endocrinology,* 142**,** 4349-56.

NAM, K. T., LEE, H. J., MOK, H., ROMERO-GALLO, J., CROWE, J. E., JR., PEEK, R. M., JR. & GOLDENRING, J. R. 2009. Amphiregulin-deficient mice develop spasmolytic polypeptide expressing metaplasia and intestinal metaplasia. *Gastroenterology,* 136**,** 1288-96.

NEVE, A., CORRADO, A. & CANTATORE, F. P. 2013. Osteocalcin: skeletal and extra-skeletal effects. *J Cell Physiol,* 228**,** 1149-53.

NICKERSON, N. K., MOHAMMAD, K. S., GILMORE, J. L., CRISMORE, E., BRUZZANITI, A., GUISE, T. A. & FOLEY, J. 2012. Decreased autocrine EGFR signaling in metastatic breast cancer cells inhibits tumor growth in bone and mammary fat pad. *PLoS One,* 7**,** e30255.

NISHIDA, S., YAMAGUCHI, A., TANIZAWA, T., ENDO, N., MASHIBA, T., UCHIYAMA, Y., SUDA, T., YOSHIKI, S. & TAKAHASHI, H. E. 1994. Increased bone formation by intermittent parathyroid hormone administration is due to the stimulation of proliferation and differentiation of osteoprogenitor cells in bone marrow. *Bone,* 15**,** 717-23.

NOJIRI, T., YOSHIZATO, T., FUKAMI, T., OBAMA, H., YAGI, H., YOTSUMOTO, F. & MIYAMOTO, S. 2012. Clinical significance of amphiregulin and epidermal growth factor in colostrum. *Arch Gynecol Obstet,* 286**,** 643-7.

ONYIA, J. E., HELVERING, L. M., GELBERT, L., WEI, T., HUANG, S., CHEN, P., DOW, E. R., MARAN, A., ZHANG, M., LOTINUN, S., LIN, X., HALLADAY, D. L., MILES, R. R., KULKARNI, N. H., AMBROSE, E. M., MA, Y. L., FROLIK, C. A., SATO, M., BRYANT, H. U. & TURNER, R. T. 2005. Molecular profile of catabolic versus anabolic treatment regimens of parathyroid hormone (PTH) in rat bone: an analysis by DNA microarray. *J Cell Biochem,* 95**,** 403-18.

OURSLER, M. J., OSDOBY, P., PYFFEROEN, J., RIGGS, B. L. & SPELSBERG, T. C. 1991. Avian osteoclasts as estrogen target cells. *Proc Natl Acad Sci U S A,* 88**,** 6613-7.

PACIFICI, R. 1996. Estrogen, cytokines, and pathogenesis of postmenopausal osteoporosis. *J Bone Miner Res,* 11**,** 1043-51.

PARTRIDGE, N. C., LI, X. & QIN, L. 2006. Understanding parathyroid hormone action. *Ann N Y Acad Sci,* 1068**,** 187-93.

PETERSON, E. A., JENKINS, E. C., LOFGREN, K. A., CHANDIRAMANI, N., LIU, H., ARANDA, E., BARNETT, M. & KENNY, P. A. 2015. Amphiregulin Is a Critical Downstream Effector of Estrogen Signaling in ERalpha-Positive Breast Cancer. *Cancer Res,* 75**,** 4830-8.

PETTWAY, G. J., MEGANCK, J. A., KOH, A. J., KELLER, E. T., GOLDSTEIN, S. A. & MCCAULEY, L. K. 2008. Parathyroid hormone mediates bone growth through the regulation of osteoblast proliferation and differentiation. *Bone,* 42**,** 806-18.

PLOWMAN, G. D., GREEN, J. M., MCDONALD, V. L., NEUBAUER, M. G., DISTECHE, C. M., TODARO, G. J. & SHOYAB, M. 1990. The amphiregulin gene encodes a novel epidermal growth factor-related protein with tumor-inhibitory activity. *Mol Cell Biol,* 10**,** 1969-81.

POOLE, K. E. & REEVE, J. 2005. Parathyroid hormone - a bone anabolic and catabolic agent. *Curr Opin Pharmacol,* 5**,** 612-7.

PRENZEL, N., ZWICK, E., DAUB, H., LESERER, M., ABRAHAM, R., WALLASCH, C. & ULLRICH, A. 1999. EGF receptor transactivation by G-protein-coupled receptors requires metalloproteinase cleavage of proHB-EGF. *Nature,* 402**,** 884-8.

QIN, L., QIU, P., WANG, L., LI, X., SWARTHOUT, J. T., SOTEROPOULOS, P., TOLIAS, P. & PARTRIDGE, N. C. 2003. Gene expression profiles and transcription factors involved in parathyroid hormone signaling in osteoblasts revealed by microarray and bioinformatics. *J Biol Chem,* 278**,** 19723-31.

QIN, L., TAMASI, J., RAGGATT, L., LI, X., FEYEN, J. H., LEE, D. C., DICICCO-BLOOM, E. & PARTRIDGE, N. C. 2005. Amphiregulin is a novel growth factor involved in normal bone development and in the cellular response to parathyroid hormone stimulation. *J Biol Chem,* 280**,** 3974-81.

QU, Q., PERALA-HEAPE, M., KAPANEN, A., DAHLLUND, J., SALO, J., VAANANEN, H. K. & HARKONEN, P. 1998. Estrogen enhances differentiation of osteoblasts in mouse bone marrow culture. *Bone,* 22**,** 201-9.

RAGGATT, L. J., QIN, L., TAMASI, J., JEFCOAT, S. C., JR., SHIMIZU, E., SELVAMURUGAN, N., LIEW, F. Y., BEVELOCK, L., FEYEN, J. H. & PARTRIDGE, N. C. 2008. Interleukin-18 is regulated by parathyroid hormone and is required for its bone anabolic actions. *J Biol Chem,* 283**,** 6790-8.

REGINSTER, J. Y., BRANDI, M. L., CANNATA-ANDIA, J., COOPER, C., CORTET, B., FERON, J. M., GENANT, H., PALACIOS, S., RINGE, J. D. & RIZZOLI, R. 2015. The position of strontium ranelate in today's management of osteoporosis. *Osteoporos Int*.

REIM, N. S., BREIG, B., STAHR, K., EBERLE, J., HOEFLICH, A., WOLF, E. & ERBEN, R. G. 2008. Cortical bone loss in androgen-deficient aged male rats is mainly caused by increased endocortical bone remodeling. *J Bone Miner Res,* 23**,** 694-704.

RIESE, D. J., 2ND & CULLUM, R. L. 2014. Epiregulin: roles in normal physiology and cancer. *Semin Cell Dev Biol,* 28**,** 49-56.

RIGGS, B. L., KHOSLA, S. & MELTON, L. J., 3RD 2002. Sex steroids and the construction and conservation of the adult skeleton. *Endocr Rev,* 23**,** 279-302.

ROODMAN, G. D. 2001. Biology of osteoclast activation in cancer. *J Clin Oncol,* 19**,** 3562-71.

SAHIN, U., WESKAMP, G., KELLY, K., ZHOU, H. M., HIGASHIYAMA, S., PESCHON, J., HARTMANN, D., SAFTIG, P. & BLOBEL, C. P. 2004. Distinct roles for ADAM10 and ADAM17 in ectodomain shedding of six EGFR ligands. *J Cell Biol,* 164**,** 769-79.

SCHMIDT, J., LUMNICZKY, K., TZSCHASCHEL, B. D., GUENTHER, H. L., LUZ, A., RIEMANN, S., GIMBEL, W., ERFLE, V. & ERBEN, R. G. 1999. Onset and dynamics of osteosclerosis in mice induced by Reilly-Finkel-Biskis (RFB) murine leukemia virus. Increase in bone mass precedes lymphomagenesis. *Am J Pathol,* 155**,** 557-70.

SCHNEIDER, M. R., DAHLHOFF, M., ANDRUKHOVA, O., GRILL, J., GLOSMANN, M., SCHULER, C., WEBER, K., WOLF, E. & ERBEN, R. G. 2012. Normal epidermal growth factor receptor signaling is dispensable for bone anabolic effects of parathyroid hormone. *Bone,* 50**,** 237-44.

SCHNEIDER, M. R., DAHLHOFF, M., HERBACH, N., RENNER-MUELLER, I., DALKE, C., PUK, O., GRAW, J., WANKE, R. & WOLF, E. 2005. Betacellulin overexpression in transgenic mice causes disproportionate growth, pulmonary hemorrhage syndrome, and complex eye pathology. *Endocrinology,* 146**,** 5237-46.

SCHNEIDER, M. R., MAYER-ROENNE, B., DAHLHOFF, M., PROELL, V., WEBER, K., WOLF, E. & ERBEN, R. G. 2009a. High cortical bone mass phenotype in betacellulin transgenic mice is EGFR dependent. *J Bone Miner Res,* 24**,** 455-67.

SCHNEIDER, M. R., SIBILIA, M. & ERBEN, R. G. 2009b. The EGFR network in bone biology and pathology. *Trends Endocrinol Metab,* 20**,** 517-24.

SCHNEIDER, M. R. & WOLF, E. 2009. The epidermal growth factor receptor ligands at a glance. *J Cell Physiol,* 218**,** 460-6.

SCHNEIDER, M. R. & YARDEN, Y. 2013. Structure and function of epigen, the last EGFR ligand. *Semin Cell Dev Biol*.

SHOYAB, M., MCDONALD, V. L., BRADLEY, J. G. & TODARO, G. J. 1988. Amphiregulin: a bifunctional growth-modulating glycoprotein produced by the phorbol 12-myristate 13-acetate-treated human breast adenocarcinoma cell line MCF-7. *Proc Natl Acad Sci U S A,* 85**,** 6528-32.

SIBILIA, M., WAGNER, B., HOEBERTZ, A., ELLIOTT, C., MARINO, S., JOCHUM, W. & WAGNER, E. F. 2003. Mice humanised for the EGF receptor display hypomorphic phenotypes in skin, bone and heart. *Development,* 130**,** 4515-25.

SIBILIA, M. & WAGNER, E. F. 1995. Strain-dependent epithelial defects in mice lacking the EGF receptor. *Science,* 269**,** 234-8.

SINGH, A. B. & HARRIS, R. C. 2005. Autocrine, paracrine and juxtacrine signaling by EGFR ligands. *Cell Signal,* 17**,** 1183-93.

SINGH, B. & COFFEY, R. J. 2014. From wavy hair to naked proteins: the role of transforming growth factor alpha in health and disease. *Semin Cell Dev Biol,* 28**,** 12-21.

SUGIYAMA, T., TORIO, T., SATO, T., MATSUMOTO, M., KIM, Y. T. & ODA, H. 2015. Improvement of skeletal fragility by teriparatide in adult osteoporosis patients: a novel mechanostat-based hypothesis for bone quality. *Front Endocrinol (Lausanne),* 6**,** 6.

SUNNARBORG, S. W., HINKLE, C. L., STEVENSON, M., RUSSELL, W. E., RASKA, C. S., PESCHON, J. J., CASTNER, B. J., GERHART, M. J., PAXTON, R. J., BLACK, R. A. & LEE, D. C. 2002. Tumor necrosis factor-alpha converting enzyme (TACE) regulates epidermal growth factor receptor ligand availability. *J Biol Chem,* 277**,** 12838-45.

SWARTHOUT, J. T., D'ALONZO, R. C., SELVAMURUGAN, N. & PARTRIDGE, N. C. 2002. Parathyroid hormone-dependent signaling pathways regulating genes in bone cells. *Gene,* 282**,** 1-17.

TAM, C. S., HEERSCHE, J. N., MURRAY, T. M. & PARSONS, J. A. 1982. Parathyroid hormone stimulates the bone apposition rate independently of its resorptive action: differential effects of intermittent and continuous administration. *Endocrinology,* 110**,** 506-12.

TAMASI, J. A., VASILOV, A., SHIMIZU, E., BENTON, N., JOHNSON, J., BITEL, C. L., MORRISON, N. & PARTRIDGE, N. C. 2013. Monocyte chemoattractant protein-1 is a mediator of the anabolic action of parathyroid hormone on bone. *J Bone Miner Res,* 28**,** 1975-86.

TAO, Y. X. & CONN, P. M. 2014. Chaperoning G protein-coupled receptors: from cell biology to therapeutics. *Endocr Rev,* 35**,** 602-47.

TAYLOR, S. R., MARKESBERY, M. G. & HARDING, P. A. 2014. Heparin-binding epidermal growth factor-like growth factor (HB-EGF) and proteolytic processing by a disintegrin and metalloproteinases (ADAM): a regulator of several pathways. *Semin Cell Dev Biol,* 28**,** 22-30.

TEITELBAUM, S. L. 2000. Bone resorption by osteoclasts. *Science,* 289**,** 1504-8.

TELLA, S. H. & GALLAGHER, J. C. 2014. Prevention and treatment of postmenopausal osteoporosis. *J Steroid Biochem Mol Biol,* 142**,** 155-70.

THREADGILL, D. W., DLUGOSZ, A. A., HANSEN, L. A., TENNENBAUM, T., LICHTI, U., YEE, D., LAMANTIA, C., MOURTON, T., HERRUP, K., HARRIS, R. C. & ET AL. 1995. Targeted disruption of mouse EGF receptor: effect of genetic background on mutant phenotype. *Science,* 269**,** 230-4.

TOMKINSON, A., GEVERS, E. F., WIT, J. M., REEVE, J. & NOBLE, B. S. 1998. The role of estrogen in the control of rat osteocyte apoptosis. *J Bone Miner Res,* 13**,** 1243-50.

USMANI, S. E., PEST, M. A., KIM, G., OHORA, S. N., QIN, L. & BEIER, F. 2012. Transforming growth factor alpha controls the transition from hypertrophic cartilage to bone during endochondral bone growth. *Bone,* 51**,** 131-41.

VAIDYA, M., LEHNER, D., HANDSCHUH, S., JAY, F. F., ERBEN, R. G. & SCHNEIDER, M. R. 2015. Osteoblast-specific overexpression of amphiregulin leads to transient increase in femoral cancellous bone mass in mice. *Bone*.

VENDRELL, J. A., MAGNINO, F., DANIS, E., DUCHESNE, M. J., PINLOCHE, S., PONS, M., BIRNBAUM, D., NGUYEN, C., THEILLET, C. & COHEN, P. A. 2004. Estrogen regulation in human breast cancer cells of new downstream gene targets involved in estrogen metabolism, cell proliferation and cell transformation. *J Mol Endocrinol,* 32**,** 397-414.

VESPER, H. W., AUDAIN, C., WOOLFITT, A., OSPINA, M., BARR, J., ROBINS, S. P. & MYERS, G. L. 2003. High-performance liquid chromatography method to analyze free and total urinary pyridinoline and deoxypyridinoline. *Anal Biochem,* 318**,** 204-11.

VON STECHOW, D., ZURAKOWSKI, D., PETTIT, A. R., MULLER, R., GRONOWICZ, G., CHOREV, M., OTU, H., LIBERMANN, T. & ALEXANDER, J. M. 2004. Differential transcriptional effects of PTH and estrogen during anabolic bone formation. *J Cell Biochem,* 93**,** 476-90.

WANG, K., YAMAMOTO, H., CHIN, J. R., WERB, Z. & VU, T. H. 2004. Epidermal growth factor receptor-deficient mice have delayed primary endochondral ossification because of defective osteoclast recruitment. *J Biol Chem,* 279**,** 53848-56.

WEBER, K., KASCHIG, C. & ERBEN, R. G. 2004. 1 Alpha-hydroxyvitamin D2 and 1 alpha-hydroxyvitamin D3 have anabolic effects on cortical bone, but induce intracortical remodeling at toxic doses in ovariectomized rats. *Bone,* 35**,** 704-10.

WEBER, K. L., DOUCET, M., PRICE, J. E., BAKER, C., KIM, S. J. & FIDLER, I. J. 2003. Blockade of epidermal growth factor receptor signaling leads to inhibition of renal cell carcinoma growth in the bone of nude mice. *Cancer Res,* 63**,** 2940-7.

WEN, Y. H., KOEPPEN, H., GARCIA, R., CHIRIBOGA, L., TARLOW, B. D., PETERS, B. A., EIGENBROT, C., YEE, H., STEINER, G. & GRECO, M. A. 2007. Epidermal growth factor receptor in osteosarcoma: expression and mutational analysis. *Hum Pathol,* 38**,** 1184-91.

WILLMARTH, N. E. & ETHIER, S. P. 2006. Autocrine and juxtacrine effects of amphiregulin on the proliferative, invasive, and migratory properties of normal and neoplastic human mammary epithelial cells. *J Biol Chem,* 281**,** 37728-37.

YARDEN, Y. & SLIWKOWSKI, M. X. 2001. Untangling the ErbB signalling network. *Nat Rev Mol Cell Biol,* 2**,** 127-37.

YU, X. P. & CHANDRASEKHAR, S. 1997. Parathyroid hormone (PTH 1-34) regulation of rat osteocalcin gene transcription. *Endocrinology,* 138**,** 3085-92.

ZAISS, D. M., GAUSE, W. C., OSBORNE, L. C. & ARTIS, D. 2015. Emerging Functions of Amphiregulin in Orchestrating Immunity, Inflammation, and Tissue Repair. *Immunity,* 42**,** 216-226.

ZENG, F. & HARRIS, R. C. 2014. Epidermal growth factor, from gene organization to bedside. *Semin Cell Dev Biol,* 28**,** 2-11.

ZHANG, X., SICLARI, V. A., LAN, S., ZHU, J., KOYAMA, E., DUPUIS, H. L., ENOMOTO-IWAMOTO, M., BEIER, F. & QIN, L. 2011a. The critical role of the epidermal growth factor receptor in endochondral ossification. *J Bone Miner Res,* 26**,** 2622-33.

ZHANG, X., TAMASI, J., LU, X., ZHU, J., CHEN, H., TIAN, X., LEE, T. C., THREADGILL, D. W., KREAM, B. E., KANG, Y., PARTRIDGE, N. C. & QIN, L. 2011b. Epidermal growth factor receptor plays an anabolic role in bone metabolism in vivo. *J Bone Miner Res,* 26**,** 1022-34.

ZHANG, X., ZHU, J., LI, Y., LIN, T., SICLARI, V. A., CHANDRA, A., CANDELA, E. M., KOYAMA, E., ENOMOTO-IWAMOTO, M. & QIN, L. 2013. Epidermal growth factor receptor (EGFR) signaling regulates epiphyseal cartilage development through beta-catenin-dependent and -independent pathways. *J Biol Chem,* 288**,** 32229-40.

ZHU, J., JIA, X., XIAO, G., KANG, Y., PARTRIDGE, N. C. & QIN, L. 2007. EGF-like ligands stimulate osteoclastogenesis by regulating expression of osteoclast regulatory factors by osteoblasts: implications for osteolytic bone metastases. *J Biol Chem,* 282**,** 26656-64.

ZHU, J., SHIMIZU, E., ZHANG, X., PARTRIDGE, N. C. & QIN, L. 2011. EGFR signaling suppresses osteoblast differentiation and inhibits expression of master osteoblastic transcription factors Runx2 and Osterix. *J Cell Biochem,* 112**,** 1749-60.

ZHU, J., SICLARI, V. A., LIU, F., SPATZ, J. M., CHANDRA, A., DIVIETI PAJEVIC, P. & QIN, L. 2012. Amphiregulin-EGFR signaling mediates the migration of bone marrow mesenchymal progenitors toward PTH-stimulated osteoblasts and osteocytes. *PLoS One,* 7**,** e50099.

9 Acknowledgements

First of all, I would like to thank my *Doktorvater* PD Dr. Marlon R. Schneider for giving me the opportunity to work on this project, for his constant support, guidance, encouragement and always valuable suggestions.

I would like to express my sincere gratitude to Prof. Dr. Dr. Reinhold Erben, Institute of Physiology, Pathophysiology and Experimental Endocrinology of the University of Veterinary Medicine, Vienna, for his support, helpful discussions and sharing his great experience.

I am indebted to Prof. Dr. Eckard Wolf for the ability to carry out this work at the Institute for Molecular Animal Breeding and Biotechnology, Gene Center, Munich, and for the excellent working conditions.

This work would not have been possible without my two co-workers Mithila Vaidya and Dr. Sabrina Porada. Thank you for your help, the many lively discussions about bone and beyond and for standing by my side throughout this challenging and suspenseful time.

I would like to extend my thanks to all my (former) colleagues at the Gene Center Munich and at the University of Veterinary Medicine, Vienna. I am especially thankful to Sepp Millauer, Christiane Schüler, Esther Erben, Anita Smolnik, and Claudia Bergow for excellent technical assistance, and to Dr. Olena Andrukhova and Dr. Ingrid Kantner for their help and support. I am particularly grateful to Dr. Maik Dahlhoff and Stefanie Riesemann for introducing me to molecular biology and teaching me the first steps in a laboratory back in 2011. Many thanks to Sylvia Hornig for her constant support and secretary training, and to Michaela Dmochewitz for her valuable advice, endless amount of patience and friendship.

Special thanks to the members of the animal maintenance group, especially Dr. Ingrid Renner-Müller and Petra Renner for their guidance, encouragement and for sharing their great experience in the field of laboratory animal welfare.

This research was supported by grants from the Deutsche Forschungsgemeinschaft and from the Austrian Science Fund.